Simulation of hadronic and electromagnetic cascades in the elements of superconducting accelerators and particle detectors at energies up to 20 TeV

N. V. Mokhov

Institute of High Energy Physics, Serpukhov

Fiz. Elem. Chastits At. Yadra **18**, 960–999 (September–October 1987)

Methods are described for simulating the interaction of relativistic particles with matter and constructing three-dimensional trajectories in geometrically complicated systems in the presence of external magnetic fields. Depending on the method used to simulate the multiparticle production events, three types of cascade calculation are considered: exclusive, quasiexclusive, and inclusive. Algorithms for calculating electron–photon showers, nuclear–electromagnetic cascades, and the production and propagation of muons in matter are considered. An analysis is made of the quality and possibilities of the existing programs used to calculate cascades in the multi-TeV energy region. Various approaches are considered, and the use of the described methods is illustrated by examples of the solution of a number of problems at the big accelerators.

INTRODUCTION

The construction of the accelerators of the new generation and experimental detection facilities of matching scales is unthinkable without mathematical simulation of the hadronic and electromagnetic cascades that arise when high-energy particles interact with the elements of these systems. Such simulation is particularly important in the stage of planning of modern experiments and in the design of superconducting proton accelerators: UNK (3 TeV) (the large accelerator planned at Serpukhov), LHC (10 TeV), and SSC (20 TeV).

As the energy and intensity of the particle beams increase, the facilities become larger and more complicated, the possibilities offered by computers and computational programs are extended, and the number of applications of methods of calculating nuclear–electromagnetic cascades increases as in an avalanche. The ring tunnels of the new accelerators are tens of kilometers long, and the error in the determination of the dimensions of the radiation shield—in some cases reaching kilometers of ground—may result in a high cost both ecological and economic. The very possibility of realizing high-intensity accelerator facilities using superconducting magnets is to a large degree ensured by calculation of the radiation heating of these magnets and the construction, on the basis of extensive calculations, of systems to protect the elements of the magnetic structure from the influence of radiation. The interaction of particle beams with total energy reaching hundreds of megajoules with the matter in the elements of the accelerators and the experimental equipment can drastically shorten the service lifetime of these elements and, unless special measures are taken, lead to their destruction. The simulation of physics experiments is one of the most rapidly developing applications. This can be seen particularly clearly in the example of the calorimeter—the basic instrument of high-energy physics. Irrespective of the nature of the problem to be solved, the type of calorimeter, or the principle of its operation, the functioning of the calorimeter depends essentially on the use of the basic properties of cascade development.

These and many other problems considered in the present paper are solved by mathematical simulation of hadronic and electromagnetic cascades in various facilities. The aim of the simulation is to establish the very possibility of realizing a particular solution, to estimate the expected result, to optimize the individual elements of the facility and the radiation and background conditions, to seek new solutions, and so forth. The simulation formalism is the Monte Carlo method, which enables one to take into account correctly all the physical processes of particle interaction with matter, calculate three-dimensional cascades in systems of almost arbitrary geometrical complexity in the presence of external magnetic and electric fields, and estimate in the most direct manner the fluctuations in the cascades. A factor of no little significance in practice is the simplicity and perspicuity of the algorithm for solving problems by the Monte Carlo method; a shortcoming of the method is its relatively slow convergence.

We regard the present paper as complementing the recently published studies of Refs. 1 and 2. The aim is to give more detailed consideration to particular simulation algorithms, to analyze the quality and possibilities of the existing programs used for full-scale calculations of cascades in the multi-TeV region of energies, and to consider new results. The main attention is devoted to calculations of cascades initiated by hadrons with energy from 0.1 to 20 TeV. The low-energy region is considered in Refs. 3 and 4 (see also Ref. 1 and the bibliography given there), and details of the simulation of electron–photon showers are considered in Refs. 1 and 5–8.

There are two key things that determine the region of applicability, possibilities, and quality of any program for simulating cascades and, ultimately, the circle of users and their relationship to the program:

1) the physical model used in the program, in the first place (for hadronic cascades) the method used to describe the multiparticle production of hadrons;

2) the geometrical module—the algorithms for constructing the particle trajectories, and the subprograms for the input and output of geometrical information.

In the present review, both of these are considered to have paramount importance in the analysis of the existing programs.

1. INTERACTIONS OF HIGH-ENERGY PARTICLES WITH MATTER

The development of nuclear–electromagnetic cascades initiated in a medium by high-energy hadrons is considered in detail in Ref. 1. Hadronic and electron–photon cascades

 0090-4759/87/050408-19$04.40

develop when ultrarelativistic particles pass through matter because of the multiple nature of the electromagnetic and strong hadron–nucleus interactions at high energies. Because of successive multiplication, an avalanche of interactions rapidly develops, reaches a maximum, and then dies away through the dissipation of energy between the participants in the cascade and the loss of energy by the charged particles on ionization and excitation of atoms. The length scale in a hadronic shower is the mean free path with respect to an inelastic nuclear interaction, $\lambda_{in} = A/N_A\sigma_{in}$, and in an electron–photon shower it is the radiation length $X_0 = t_r$, which is approximately determined by the expression $t_r^{-1} = 4\alpha r_0^2 Z,(Z+1)\ln(183Z^{-1/3})\rho N_A/A$. Here, A, Z, and ρ are the mass number, atomic number, and density of the matter, N_A is Avogadro's number, σ_{in} is the cross section of inelastic interaction of the hadron with a nucleus, and α and r_0 are the fine-structure constant and the classical radius of the electron.

Electromagnetic interactions entirely determine the development of the electron–photon showers and the passage of muons through matter, and they play an important part in the development of hadronic cascades. As it moves through a medium, a charged particle loses energy on the ionization and excitation of atoms, on bremsstrahlung, and on the direct production of e^+e^- pairs in the field of a nucleus and the atomic electrons. As a result of multiple Coulomb scattering, such a particle undergoes significant changes of direction of its motion. The main processes of photon interaction with matter are Rayleigh scattering, the photoelectric effect, the Compton effect, and the production of e^+e^- pairs. Methods for simulating all these processes are described in detail in, for example, Refs. 1, 5–7, and 9–11.

At energy $E \lesssim 100$ GeV for particles heavier than the electron, the main electromagnetic processes are ionization and excitation of atoms and multiple Coulomb scattering. At higher energies, the importance of other processes is much greater.[1,9] Figure 1 shows the distribution functions with respect to the energy losses $V = (E_0 - E)/(E_0 - m)$

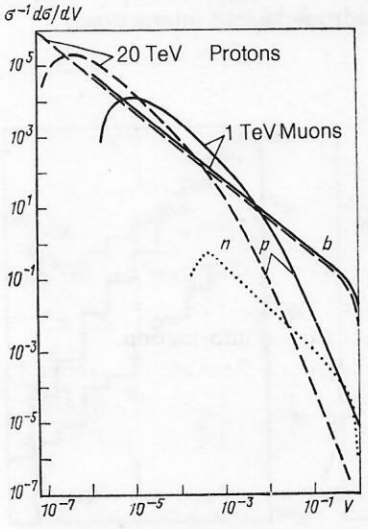

FIG. 1. Universal differential distributions with respect to the energy losses for protons and muons in the following processes: bremsstrahlung (b), direct production of e^+e^- pairs (p), and deep inelastic muon scattering (n).

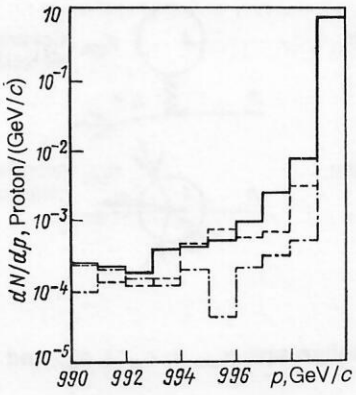

FIG. 2. Momentum distribution calculated by MARS10 for protons emerging from tungsten wires of the electrostatic deflector of the Tevatron with which part of the proton beam with momentum $p_0 = 1$ TeV/c interacts. The solid histogram is the complete simulation of all processes; the broken histogram is without allowance for fluctuations in the process of e^+e^- pair production; and the chain histogram is without allowance for Landau fluctuations in the e^+e^- pair-production process.

in different processes for high-energy protons and muons as calculated in Ref. 10. For muons with energy above a few hundred giga-electron-volts, especially in heavy media, the angular deflections due to the emission of bremsstrahlung photons begin to dominate over multiple Coulomb scattering,[11] and the energy losses are determined by bremsstrahlung and direct production of e^+e^- pairs.

For particles heavier than the muon, this occurs at higher energies and does not strongly affect the development of the complete hadronic cascade. However, in a number of problems (energy release near the beam axis and particle scattering by thin structures), bremsstrahlung and the direct production of e^+e^- pairs must be described as discrete processes for proton beams already at an energy around 1 TeV. This fact, discovered in Refs. 12 and 13, appeared in calculations of the azimuthal distributions of the beam losses and in the development of measures to shield superconducting magnets from irradiation at energy 3 TeV in the UNK (Ref. 14) and 1 TeV in the Tevatron.[15] Figure 2, which shows the part of the momentum spectrum of protons emerging from a tungsten electrostatic septum magnet that is important for calculations of the beam losses, clearly illustrates the importance of correct simulation of the process of direct production of e^+e^- pairs by protons and the fluctuations of the ionization losses.

Detailed information about processes of multiparticle production of hadrons on nucleons and nuclei at $E_0 > 10$ GeV can be found in the monographs of Refs. 1 and 16–18 and the reviews of Refs. 19 and 20. All hadron–nucleus (hA) interactions can be divided into two groups:

1) elastic, without the production of new particles,

$$h + A \to h + A; \tag{1}$$

2) inelastic, with production of at least one particle not present in the initial state,

$$h + A \to c + d + \ldots + f. \tag{2}$$

Each of these groups, in turn, can be subdivided into two parts—coherent and incoherent (Fig. 3). The cross section of each of the reactions (1) and (2) is determined as the sum

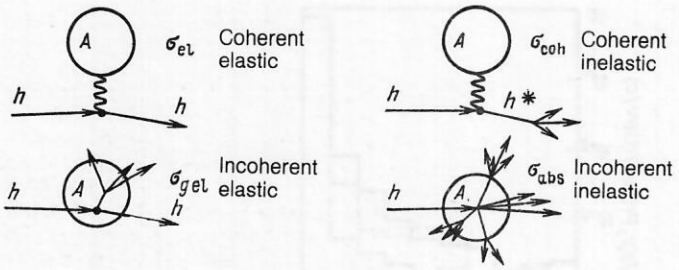

FIG. 3. Different type of hadron–nucleus interaction.

of the cross sections in the subgroups: $\sigma_{scat} = \sigma_{el} + \sigma_{qel}$ and $\sigma_{prod} = \sigma_{coh} + \sigma_{abs} = \sigma_{in}$.

The process of incoherent elastic (quasielastic) scattering should, strictly speaking, be included with the inelastic processes.[3] For the development of hadronic cascades, it is important that in the fourth of the processes in Fig. 3 there is an energetically distinguished leading particle.

In the tera-electron-volt region of energies the multiplicities of the secondary particles in the reaction (2) are very high even in hN collisions (Fig. 4). For nuclei, the mean multiplicity of fast ($\beta > 0.7$) particles is $\langle N_s \rangle_A \simeq \langle n_c \rangle_{hN} (0.4 + 0.6A\sigma_{in}^{hN}/\sigma_{abs}^{hA})$. All this has the consequence that the cascade acquires exceptionally many branches already for small matter thicknesses, and this leads inevitably to many computational problems.

2. DESCRIPTION OF HADRON–NUCLEUS INTERACTIONS

As already noted in the Introduction, a central question in all programs for simulating hadronic cascades is the method of describing the processes of multiple production of hadrons in hA interactions. It is this that basically determines the energy range of the program, the group of physical problems to which it can be applied, and the agreement between the results and reality, and it also significantly affects the speed of the program and its popularity among users.

In the overwhelming majority of applications considered in the present study, the important range of kinetic energies of the hadrons in the cascade extends from a few mega-electron-volts to a primary energy $E_0 \lesssim 20$ TeV. A unified theoretical model for the complete range of variation of the kinematic variables in this complete interval of energies does not exist. Therefore, in the majority of cases one uses combinations of particular theoretical constructions with phenomenological descriptions.

We briefly consider the existing algorithms for simulating multiparticle production of hadrons developed in the framework of programs for calculating hadronic cascades or independently. Since we are interested in models that give the information needed for continuous calculation of cascades in the complete range $10^{-2} < E_0 < 10^4$ GeV, so far as possible with uniform reliability, we shall not consider the following algorithms: the intranuclear-cascade model,[3,4] which has proved very satisfactory at energies $E_0 \lesssim 30$ GeV and is the basis of the well-known programs SHIELD (Ref. 24) and HETC (Ref. 25); the constructions lacking the required generality, used in cosmic-ray physics (see, for example, Ref. 26) and in applications to calorimeters,[27,28] and some others.

The most popular programs for generating hadron interactions are at present LUND (Ref. 21) and ISAJET (Ref. 22). The program ISAJET uses quantum chromodynamics augmented by a fragmentation model that treats all partons in an event as independent. In this model, the energy, momentum, and flavor conservation laws are not satisfied explicitly. The program LUND is based on a string model with gluons, which arise as perturbations in the strings joining the partons in a high-energy event. In this case, fulfillment of the conservation laws is ensured. Both programs have a number of free parameters and do not describe very well the region of small transverse momenta.[23] However, they enable one to simulate all the main features of the interactions in the tera-electron-volt region of energies, they agree well with the experimental data, and the results of calculations by the two programs largely agree (see Fig. 4). There is good hope of successful use of these programs to generate events for the planned colliders and as a basis for programs of simulating hadron–nucleus interactions.

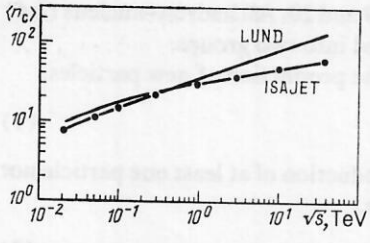

FIG. 4. Mean multiplicity of charged particles in a pp collision calculated using the programs LUND (Ref. 21) and ISAJET (Ref. 22) and plotted as a function of the interaction energy. The black circles represent the approximation in Ref. 18 of the experimental data by $\langle n_c \rangle = 0.88 + 0.44 \ln s + 0.118 \ln^2 s$, where s is measured in GeV^2.

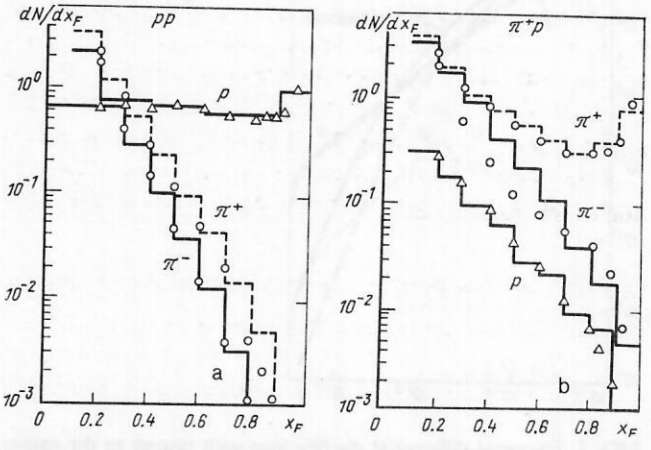

FIG. 5. Distributions of hadrons with respect to $x_F = 2p_\parallel^*/\sqrt{s}$ in pp and $\pi^+ p$ interactions at energy 100 GeV calculated by the program MARS10. The points represent the experimental results of Ref. 38.

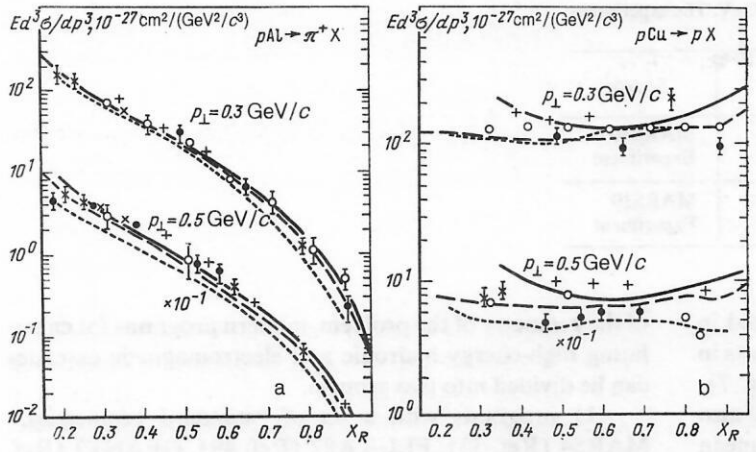

FIG. 6. Invariant cross sections of the reactions $pAl \to \pi^+ X$ and $pCu \to pX$ at two values of the transverse momentum, $x_R = E^*/E^*_{max}$. Calculations: the continuous curve for $p_0 = 19.2$ GeV/c, MARS10; the broken curve for $p_0 = 100$ GeV/c, MARS10; the dotted curve for $p_0 = 100$ GeV/c (Ref. 30) and the nuclear algorithm from MARS10. The experiments: the plus signs are for $p_0 = 19.2$ GeV/c (Ref. 40); the crosses for $p_0 = 24$ GeV/c (Ref. 41); the black circles for $p_0 = 69$ GeV/c (the data of Ref. 42, multiplied by two); the open circles for $p_0 = 100$ GeV/c.[39]

Reliable Soviet programs have been developed for simulating multiparticle production in high-energy hadron–nucleon and hadron–nucleus collisions:

1) a method[29] based on the additive quark model in which, in accordance with quark–hadron duality, the interaction of the constituent quarks with the nuclei is reduced to a definite sequence of interactions of hadrons with nucleons of the nuclei; the Monte Carlo procedure ascribes to each such interaction, with the necessary weight, an exclusive final state, which is also described by the statistical simulation;

2) the program of Ref. 30, based on Monte Carlo sampling of particle characteristics from the phenomenological two-dimensional inclusive distributions obtained by the authors in inelastic hadron–nucleon collisions;

3) the method of Ref. 31, in which intranuclear cascades with quark–gluon strings are calculated in the framework of the dual parton model.

These programs reproduce well the characteristics of multiparticle production of hadrons in the range 5 GeV $\leqslant E_0 \leqslant$ 5 TeV of energies of the primary particles.

The package of programs in the complex MARS (Refs. 1, 2, 12, 32, and 33) is designed for the calculation of hadronic cascades. It is based on statistical simulation of the inclusive characteristics of hadron–nucleus interactions using a phenomenological construction that describes the complete range of kinematic variables in the range of primary energies 10 MeV $\leqslant E_0 \leqslant$ 30 TeV. At $E_0 > 5$ GeV, the sampling is realized by means of a system of phenomenological formulas for a hydrogen target (see Ref. 1). The transition to a nucleus is based on the predictions of the additive quark model[20,34] at $x_F > 0$ and on the phenomenological model of Ref. 35 for $x_F \leqslant 0$; here, $x_F = 2p^*_\parallel/\sqrt{s}$ is the Feynman variable. The production of slow nucleons,[36] evaporation of the nucleus, and the production of diffraction particles are simulated separately. At $E_0 \leqslant 5$ GeV, the simulation is based on the approximations of Ref. 37. In Figs. 5 and 6 we compare with experiment[38–42] the inclusive spectra of hadrons on hydrogen and nuclear targets calculated using the program MARS10. The mean characteristics obtained by MARS10, given in Tables I and II for $E_0 = 100$ GeV, also agree well with the experimental data.

Single-particle inclusive distributions are also used to simulate hadron–nucleus interactions in the programs FLUKA (Ref. 45), KASPRO (Ref. 46), and CASIM (Ref. 47), though with different generation algorithms and narrower ranges of the kinematic variables than in the MARS complex. In the program CASIM, the inclusive spectra of fast particles are described in the framework of the thermodynamic model of Hagedorn and Ranft,[48] and the characteristics of slow particles are sampled in accordance with the formulas of Ref. 36.

The method realized in the program FLUKA82 (Ref. 49) and the simple but effective method of the program GHEISHA (Ref. 50) provide reliable schemes for exclusive generation of hadron–nucleus collisions. In the method of Ref. 49, the production of particles in the range 50 MeV $< E_0 <$ 5 GeV is described by means of quasi-two-particle processes with successive decays of produced resonances. In the interval of primary energies 5 GeV $< E_0 <$ 10 TeV, the method is based on the scheme of dual topological unitarization, which treats the production of particles in hadron–nucleus interactions as fragmentation of quark–antiquark, quark–diquark, and diquark–antidiquark pairs. Strict fulfillment of the conservation laws for energy, momentum, and all the additive quantum numbers is ensured in the model. However, the production of low-energy cascade nucleons is described phenomenologically.

In the method of Ref. 50, which is designed for the calculation of hadronic cascades in calorimeters at energies E_0

TABLE I. Mean multiplicity $\langle N_s \rangle$ of shower particles in $\pi^- A$ interactions at $E_0 = 100$ GeV.

Source	p	C	Cu	Pb
Experiment[43]	6.5±0.4	8.4±0.7	10.6±0.9	12.6±1.1
MARS10	7.1	8.9	11.2	14.0
HETC[44]	1.88	10.4	14.7	20.1

TABLE II. Mean partial inelasticity coefficients $\langle K_j \rangle$ at $E_0 = 100$ GeV. The experimental data are taken from Ref. 20.

Interaction	p	π^+	π^-	π^0	Source
$\pi^+ p$	0.03 0.04	0.41 0.45	0.22 0.21	0.31 0.29	MARS10 Experiment
π^+C	0.04 —	0.39 0.37	0.24 0.24	0.31 0.31	MARS10 Experiment

<0.5 TeV, the hadron–nucleus collision is constructed in accordance with a fast algorithm,[50–54] which gives results in reasonable agreement with the experimental data (Fig. 7). Figure 8 gives a result obtained in this scheme that will also be of interest in subsequent applications, namely, the mean total kinetic energy of the secondary particles as a function of the energy of a pion that interacts with different nuclei.

3. THE GEOMETRY AND SIMULATION OF THE PARTICLE TRAJECTORIES

Experience shows that the users of programs for calculating cascades are usually not interested in the details of the physical model, especially if the calculated result is "physically reasonable," but are interested primarily in the possibilities of the geometrical module. This usually consists of the following main subprograms[55,56]: 1) specification of the geometry—the input and preparation of the initial data; 2) sampling of initial coordinates of the particles in accordance with a given distribution of sources; 3) construction of particle trajectories with simulation of the quasicontinuous processes and the effect of external electromagnetic fields; 4) calculation of the volumes of zones (if necessary), and extraction of the geometrical information.

The quality of these subprograms, that is, the possibility of describing geometrically complicated systems as simply as possible and automatically and the speed of the trajectory-construction block, is decisive in the practice of simulating cascades in the elements of accelerators and detection facilities.

According to the approach adopted to the description of the geometry of the problem, modern programs for calculating high-energy hadronic and electromagnetic cascades can be divided into two groups:

1) programs with a set of "standard geometries," MARS4 (Ref. 33), FLUKA82 (Ref. 49), GEANT3 (Ref. 57), in which one can relatively easily, from a given list of different geometrical figures (surfaces), construct the complete investigated system;

2) programs with a restricted set of standard geometries, MARS9, MARS10 (Refs. 1, 2, 12, and 56), GHEISHA (Ref. 50), or with a single geometry of "continuous cylinder" type, CASIM (Ref. 47), EGS3 (Ref. 5), SIMEX1 (Ref. 7), in which the user specifies arbitrary geometries in special USER subprograms.

Programs of the first group do not require special familiarity with their structure or programming ability of the user, and in some cases they have a well-automated input and output, and this reduces the probability of errors. However, they are cumbersome, and the creation of such a program (collection of elementary volumes and the organization of the combinatorial geometry and the interfaces for different types of volumes) is a very major undertaking.

When working in the "standard" regime, the programs of the second group are analogous to those of the first, but often essential use is made of *a priori* information about the calculated geometry. In some cases, this makes them faster programs. For example, the calculations in Ref. 57 of electron–photon showers in cylindrical absorbers showed that the highly universal geometrical module of the program GEANT3 is approximately two times slower than the simple

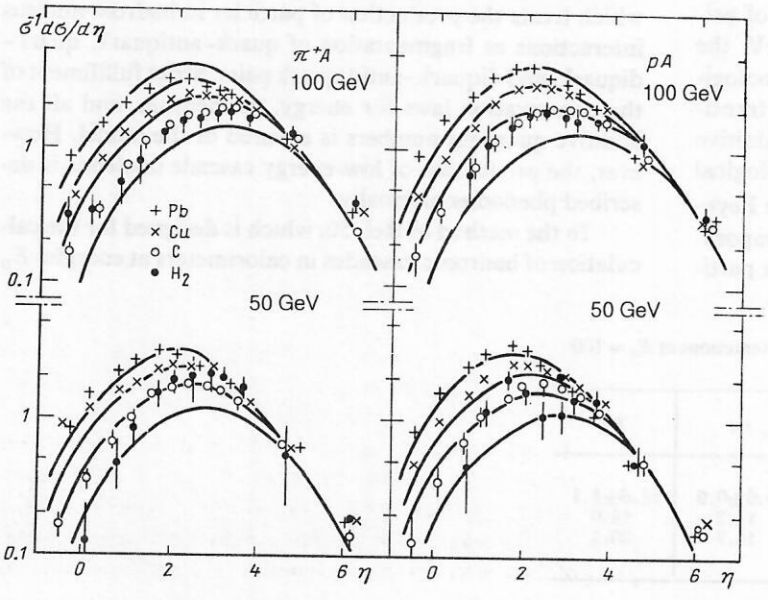

FIG. 7. Calculations by the GHEISHA program[50] of the distribution with respect to the pseudorapidity of shower particles ($\beta > 0.85$) in $\pi^+ A$ and pA collisions at energies 50 and 100 GeV. The points are the experimental data of Ref. 39.

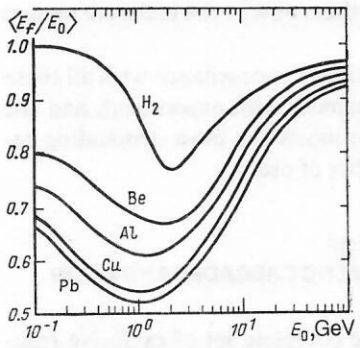

FIG. 8. Total kinetic energy of particles produced in πA interactions with energy E_0.

module of the program EGS3 in the considered case. The geometry of systems of arbitrary complexity can be specified in the USER subprograms, and here much depends on the qualifications of the user—a subprogram can be written for a particular problem much more effectively than any program of the first group and vice versa. In addition, the USER programs are a source of possible errors and it is necessary, as, in fact, is always the case, to test the given geometry.

The speed and possibilities of the geometrical module are to a large degree determined by the method of constructing the three-dimensional particle trajectories. In the majority of programs for calculating cascades, a step method is used, in which one can readily and naturally simulate quasicontinuous physical processes in strongly inhomogeneous media. One of the principal advantages of the method is that it is not necessary to calculate the coordinates of the points of intersection of a trajectory with the surfaces; instead, it is sufficient merely to determine whether a segment of a trajectory belongs to a particular zone, and this is much simpler and can be done faster.

We consider the effective algorithm for trajectory simulation in the geometrical module REGION of the MARS10 complex of programs. In the standard step method, any boundary is localized to an accuracy of the step length l. The use everywhere of large values of l leads to a distortion of the picture of the transport process that is more serious, the greater the nonuniformity of the medium. But the use of small values, as in many programs, leads to a very considerable increase in the computing time. There was therefore developed the following iterative algorithm,[56] the original variant of which is described in Refs. 1 and 13.

It is assumed that the investigated system is divided into physical zones with piecewise constant properties and material with number i. Each of the physical zones can be divided into an almost arbitrary number of geometrical zones with number N. The subprogram REGION constructs the section of a particle trajectory (path) between two collisions that are any discretely considered events. Processes with small energy transfers (some of the electromagnetic losses) are grouped together and treated as continuous. The simulation begins with the determination of the initial i and N and sampling of the range R (for charged particles, see the algorithm of Refs. 1 and 33). From the point $\mathbf{r}$ of the start of the section of the trajectory a step is taken in the direction $\mathbf{\Omega}$ of motion of the particle of length

$$l = R/L, \qquad (3)$$

where $L = \max\{1, \lambda/t\}$ for neutral particles, while for charged particles one takes into account additionally the conditions of a minimum of the error of the broken-spiral method and the error of the difference scheme for calculations in a magnetic field, and the conditions of smallness of the energy loss and applicability of the algorithm for calculating multiple Coulomb scattering; here, λ is the mean free path, and t is the length of the characteristic zone in the direction of predominant propagation of the particles.

If the point $\mathbf{r}' = \mathbf{r} + l\,\mathbf{\Omega}$ is in the same zone N, then after simulation of the effect of the magnetic field $\mathbf{B}$ and the multiple Coulomb scattering, $\mathbf{\Omega} \to \mathbf{\Omega}'$, the calculation is passed back from the subprogram.

If one of the surfaces bounding zone N has been intersected, i.e., $N' \neq N$, then to localize the point of intersection of the section of the trajectory with this surface with preassigned error ε the following algorithm is realized:

1) $n = 1$, $l_0 = l$, $\mathbf{r}_0 = \mathbf{r}$ are determined;

2) from the point $\mathbf{r}_{n-1}$ the step $l_n = l_{n-1}/2$ is taken;

3) $\mathbf{r}_n = \mathbf{r}_{n-1} + l_n\,\mathbf{\Omega}$ is calculated, and a test is made to determine whether this point belongs to zone N;

4) if it does, then n is increased by unity, step 2 is repeated, etc.; otherwise, $\mathbf{r}_n = \mathbf{r}_{n-1}$ is redetermined, n is increased by unity, and the process is continued from 2;

5) the procedure is repeated m times until $l_m = l\,2^{-m}$ becomes less than the given $\varepsilon > 0$ and the point $\mathbf{r}_n$ leaves for the first time zone N and enters its neighbor;

6) the number N' of this zone and its material number k are determined, and a new $\mathbf{\Omega}'$ is simulated.

The distance of the point $\mathbf{r}_m$ from the boundary of the zone does not exceed ε, and the length of the section of the trajectory in zone N, summed in the process of the iterations, is

$$s = l \sum_{n=1}^{m} 2^{-n} \delta_{NN'}(n), \quad \delta_{NN'} = \begin{cases} 1, & N = N', \\ 0, & N \neq N' \end{cases}$$

The total number of iterations is small, $M \simeq \ln(l/\varepsilon)/\ln 2$.

In zone N, the continuous energy losses in segment s are calculated, and contributions to the calculated functionals are made. The residual range is calculated:

$$R' = \alpha\,(R - s),$$

where

$$\alpha = \begin{cases} 1, & i = k \\ \Sigma_i(E')/\Sigma_k(E'), & i \neq k, \end{cases}$$

$\Sigma_i(E')$ is the macroscopic cross section for interaction of the particle in zone i, and E' is the energy of the particle as it enters zone k. To construct the section of the trajectory of length R', the entire procedure described above is repeated from the beginning, step 3 being changed if necessary.

In this iterative method, the error in the determination of the majority of the functionals Φ is related to ε by $\Delta\Phi/\Phi \sim \varepsilon/l$, where l is the mean total path of the particle in the given zone. Specifying the error $\Delta\Phi/\Phi$, one can then readily estimate the value of ε.

The action of the magnetic field $\mathbf{B}$ in step s is calculated in accordance with known relations.[1,56] The multiple Coulomb scattering in the same step is simulated either in the diffusion Gaussian approximation with simultaneous sampling of the transverse displacements,[56,57] or without simula-

tion of the transverse displacement using the Molière distribution, as was done in Ref. 5, or, preferably, by the algorithm of Ref. 58, based on the theory of Molière, modified to take into account the difference between the electric field of a nucleus and the field of a point charge.

4. ELECTRON–PHOTON SHOWERS

The electron–photon shower is a process that has by now been theoretically and experimentally studied in detail. There is now much interest in applying the developed methods, specifically programs for calculating showers, in the practice of experimental high-energy physics (electromagnetic calorimeters) in the solution of a number of applied problems in accelerators, and in programs of combined calculation of electron–photon showers and hadronic cascades. We shall briefly consider the state of this art. A description of the development of electron–photon showers and algorithms for simulating the electromagnetic processes of interaction can be found, for example, in Refs. 1, 5–8, and 59–62.

Many programs have been developed for Monte Carlo simulation of electron–photon showers. At the physical level, these programs in their present state differ little—one simulates the processes of bremsstrahlung, e^+e^- pair production, ionization energy losses, multiple Coulomb scattering, e^+e^- scattering by electrons, annihilation of positrons into two photons, the Compton effect, and the photoelectric effect on the K shell. The differences are usually in the methods of describing the processes of transport of low-energy electrons, the multiple Coulomb scattering, the fluctuations of the energy losses, and the allowance for, or neglect of, the Landau–Pomeranchuk–Migdal (LPM) effect. The electrons are usually followed to an energy of about 1 MeV, and the photons to 100 keV. The maximal energy is most often $E_0 \sim 100$ GeV and after allowance has been made for the LPM effect one is restricted only by the computing possibilities.

We list the main programs currently used in the Soviet Union and abroad:

1) EGS3 (Ref. 5) and EGS4 (Refs. 63 and 64)—programs that set an international standard by virtue of their universality, convenience of use, accessibility, and excellent documentation;

2) GEANT3 (Ref. 57)—a program that possesses the most powerful geometrical module among all the programs for calculating electron–photon showers, in which the physical module is identical to EGS3 with a number of simplifications;

3) AEGIS (Ref. 65)—a program designed for simultaneous calculation of nuclear–electromagnetic cascades and works in the inclusive regime (see the following section), a modified version of which is contained in the MARS10 complex;

4) the programs of the Siberian school,[6,61] which give a very detailed description of the interaction processes, especially at low energies, and a synthesis with numerical solutions that makes possible a calculation in homogeneous media at very high energies;

5) SIMEX1 (Ref. 7), RAINMC (Ref. 60), ELSS1 (Ref. 62), which provide a reliable calculation of electron–photon showers even on a computer with small memory in the analog regime, the first two of them now in the inclusive regime as well.

The results of calculations in accordance with all these programs are in good agreement with experiment, and the quality of the best of them meets the most demanding requirements of a large number of users.

5. INCLUSIVE SIMULATION OF NUCLEAR–ELECTROMAGNETIC CASCADES AND MUON PRODUCTION

The description of the complete set of exclusive reactions (2) needed to simulate hadronic cascades of tera-electron-volt energy is an exceptionally complicated problem. With increasing energy, the many-particle channels become more and more important, and the partial cross sections of each individual channel decrease to very small values. Significant progress in the analysis of multiparticle processes was achieved after recognition of the fact that a significant fraction of the information about the many-particle reaction (2) can be obtained by studying the distributions of just one of the secondary particles[66–69]:

$$h + A \to c + X, \tag{4}$$

where X is an arbitrary system of undetected particles produced together with particle c. The inclusive reaction (4) is characterized by the single-particle differential cross section

$$E_c\, d^3\sigma/dp_c^3 = f(\mathbf{p}_c;\ s), \tag{5}$$

where $\mathbf{p}_c$ is the momentum of particle c, and s is the square of the total energy of the colliding particles.

The ideology of Refs. 66–68 led to the creation of inclusive schemes for calculating hadronic and electromagnetic cascades. The stimuli were the following:

1) in the overwhelming majority of applications one considers effects due to the action of large ensembles of primary particles, so that to describe a cascade it is sufficient to have the first moment of the distribution function, obtained by means of (5), without simulating all the reactions (2);

2) at a high primary energy and low threshold energy, the tree of trajectories of the exclusive nuclear–electromagnetic cascade acquires so many branches that the calculation of a number of functionals in extended systems becomes impossible for the majority of computers;

3) the description of the complete range of variation of the kinematic variables in a wide range of primary energies is much more surely guaranteed by experimental data on inclusive spectra than by exclusive distributions.

The algorithms of inclusive simulation of cascades are based on the method of statistical weights, and this makes it possible to use devices of essential sampling for problems that are not amenable to direct calculation, for example, the investigation of low-probability reaction channels.[1] The time required to calculate one history increases with the energy only logarithmically, in contrast to exclusive programs, for which the growth is linear. This makes it possible to solve a large group of applied problems (see below) and advance into the region of arbitrarily high energies.

The price to be paid for these advantages is the impossibility of directly using the existing inclusive programs to solve the problem of the fluctuations of individual cascades in thin detectors and calorimeters, though the paper of Ref.

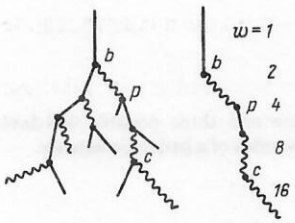

FIG. 9. Exclusive and inclusive schemes of an electron–photon shower. A continuous line represents e^+ or e^-, and a wavy line is a photon; b represents bremsstrahlung, p is the production of e^+e^- pairs, and c is the Compton effect.

71 considers an approach to the solution of this problem based on the use of an equation of Kolmogorov–Chapman type and shows that one can make an unbiased estimate of the second moment of the distribution function by means of a random process that branches less strongly than the real process.

The inclusive scheme for calculating electron–photon showers is the clearest and simplest in realization. The first program of this type was AEGIS.[65] Figure 9 shows the transition from analog simulation to calculation of a nonbranching process. Also given are the statistical weights of the particles of each generation in the simplest case when the sampling function $S(j, E_j)$ for the energy E_j is equal to the differential cross section of the process, normalized to unity, at each vertex $P(E_j)$ and the particle species j is sampled. Then

$$S(j, E_j) = \frac{1}{2} P(E_j). \tag{6}$$

The statistical weight of the particle,

$$w = P(E_j)/S(j, E_j) = \sigma^{-1} \frac{d\sigma}{dE_j} \Big/ S(j, E_j), \tag{7}$$

is in this case $w = 2$, and this doubles the weight of the simulated branch after each interaction.

It is obvious that for a large number of samplings the two schemes of Fig. 9 will give the same result. The essential sampling method immediately suggests a modification that significantly raises the efficiency of the calculation, namely, the introduction of a bias linear in the energy to equalize the probabilities of production of high-energy and low-energy particles:

$$S(j, E_j) = P(E_j) E_j/E_0. \tag{8}$$

The statistical weight in this case, $w = E_0/E_j$, ensures energy conservation at each vertex: $wE_j = E_0$.

This scheme is very compact and at the present time is included in the majority of programs for calculating electron–photon showers and in the programs CASIM and MARS for calculating nuclear–electromagnetic cascades. An example of the calculation of a cascade initiated by a 10-GeV electron in a drift calorimeter with lead glass tubes[63] is given in Fig. 10 for the exclusive and inclusive modes of the program EGS4. The radical shortening of the computing time on the transition to the inclusive regime is noteworthy.

A more correct criterion for comparing different computational schemes is the time-consumption factor $t_0 D\xi$, where t_0 is the mean time required to calculate one realization, and $D\xi$ is the dispersion of the estimate of the functional ξ. In Fig 11, taken from Ref. 72, we give the results of such investigations for an electron–photon shower initated by photons with an energy above 10 GeV in air. The threshold energy for e^+, e^-, and γ is $E_{th} = 4$ MeV. Three schemes for shower calculation were studied: 1) direct simulation (the figure gives the results of extrapolation to the high-energy region); 2) the scheme of the authors of Ref. 72 based on synthesis of the results of numerical calculations in a homogeneous medium with direct simulation; 3) the inclusive scheme. It can be seen that at high energies the inclusive scheme is more than an order of magnitude more effective than the exclusive scheme for calculating the spatial distribution of the particles. However, for calculating the total range of charged particles the direct simulation is preferable.

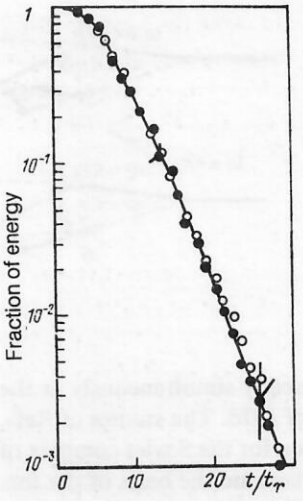

FIG. 10. The fraction of the energy of an electron–photon shower initiated by an electron with $E_0 = 10$ GeV that emerges from a calorimeter as a function of its thickness.[63] The curve represents an exclusive calculation in accordance with EGS3 (8.62 sec/history); the black circles represent an inclusive calculation in accordance with EGS4 (0.031 sec/history); the open circles represent a calculation in accordance with EGS4 in the inclusive regime for thicknesses $t \leqslant 11X_0$ and in the exclusive regime for greater thicknesses (0.045 sec/history).

The possibility of using the method of statistical weights to simulate high-energy hadron–nucleus interactions was noted in Ref. 73. The first communications of working inclusive programs for calculating hadronic cas-

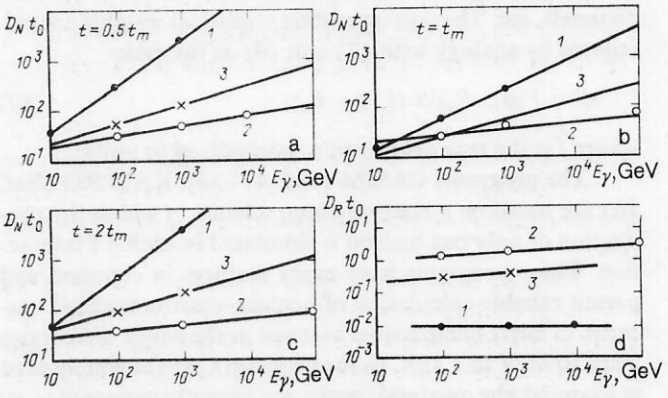

FIG. 11. Time-consumption factor for calculation of the mean number of charged particles of an electron–photon shower at depth t (a–c) and total range of the charged particles (d) as functions of the energy of the primary photon (t_m is the depth of the cascade maximum).

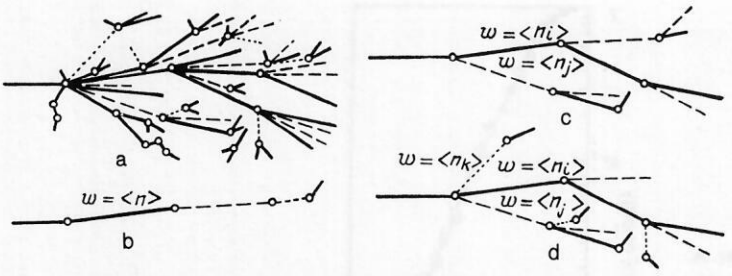

FIG. 12. Exclusive scheme and three possible inclusive schemes of the tree of trajectories of a hadronic cascade.

cades in matter appeared practically simultaneously at the end of 1974 and the beginning of 1975. The studies of Refs. 32, 74, and 75 laid the foundation for the Soviet complex of programs MARS, and Ref. 47 became the basis of the foreign inclusive program CASIM. Somewhat later, one further program for inclusive simulation of hadronic cascades, KASPRO (Ref. 46), from the FLUKA family, appeared.

Figure 12a shows the tree of trajectories of a hadronic cascade in a medium, its complete exclusive calculation being made by direct simulation. The use of the method of statistical weights to describe each *hA* interaction makes it possible to go over to processes that branch less strongly than the original one (Figs. 12c and 12d), or, as in the case of the modified calculation of electron–photon showers, do not branch at all (Fig. 12b). The statistical weights given next to each trajectory emanating from the primary vertex correspond to the simplest situation in which the sampling function is equal to the single-particle cross section (5). In this case, the weights are equal to the partial mean multiplicities of particles of species l in an *hA* collision with energy E_0,

$$w = \langle n_l \rangle = \sigma_{\text{in}}^{-1}(E_0) \int f(\mathbf{p}_l;\ E_0)\, d^3p_l/E_l, \tag{9}$$

and for a nonbranching process they are equal to the total multiplicity $w = \Sigma_l \langle n_l \rangle = \langle n \rangle$. It was proved rigorously in Ref. 71 that such an estimate of the first moment of the distribution function is unbiased.

In the general case, the sampling function $S(l, \mathbf{p}_l; E_0)$ is not necessarily identical to the real inclusive distribution. Depending on the problem, it can be chosen in such a way as to increase the weight of certain regions of the phase space: large $p_\perp$, the backward hemisphere, energies near E_0, the acceptance angles of the detector, low-probability reaction channels, etc. The corresponding statistical weights are calculated by analogy with (7) and (9) as the ratio

$$w = \hat{f}(\mathbf{p}_l;\ E_0)/S(l,\ \mathbf{p}_l;\ E_0), \tag{10}$$

where $\hat{f}$ is the true distribution, normalized to unity.

The programs CASIM (Ref. 47) and KASPRO (Ref. 46) are based on a nonbranching scheme in which the production of only one hadron is simulated in each *hA* interaction. These programs have many features in common and permit reliable calculation of nuclear–electromagnetic cascades in fairly complicated systems in the range of energies from 50 MeV to 1 TeV. In the program CASIM widely used at Fermilab the maximal energy was recently increased to 30 TeV. At the present time, both programs make it possible to calculate electron–photon showers during the development of the hadronic cascade—CASIM is combined with the program AEGIS (Ref. 65), and KASPRO with EGS3 (Refs. 5 and 76).

In the programs of the MARS complex, the possibilities of the physical and geometrical modules are extended from version to version. By means of the early versions one could investigate in detail the main features in the development of high-energy nuclear–electromagnetic cascades and solve a number of important applied problems: MARS2 (Refs. 32 and 74), MARS3 (Ref. 75), MARS4 (Ref. 33), MARS5 (Ref. 77), MARS6 (Ref. 78), MARS7 (Refs. 79 and 80). In the program MARSHI (Ref. 81) there is a synthesis of the inclusive method at high energies and the exclusive method (intranuclear-cascade model) at intermediate energies. The creation of the program MARSU made it possible to simulate the deep-water experiment DUMAND at energies up to 10^7 GeV.[70] Quasidirect simulation of electron–photon showers using a modified AEGIS algorithm is included in the program MARS8 (Ref. 80).

The modern versions of the MARS complex are the programs MARS9 (Refs. 1, 12, and 13), MARS10 (Ref. 2), and MARS11 (Ref. 82). Details of the physical model and the geometrical module of the two last programs are described in Secs. 2 and 3 of the present paper, and some aspects are described in Refs. 56 and 58. This system of programs makes it possible to calculate nuclear–electromagnetic cascades in an essentially arbitrary geometry in the presence of any large or small inhomogeneities and external electric and magnetic fields. The energies of the primary particles are in the range 10 MeV$\leqslant E_0 \leqslant$30 TeV. The charged hadrons and muons are followed down to energies 1–10 MeV, and neutrons to the same threshold (but in MARSll to 0.025 eV); the electrons are followed down to 1 MeV, and the photons to 0.1 MeV. Processes of production by hadrons and muons of direct e^+e^- pairs, bremsstrahlung, and δ electrons are simulated as discrete events. In the package MARTUR (Ref. 13), designed to calculate cascades in complicated magnetic structures of accelerators, a synthesis with the well-known program TURTLE (Ref. 83) is realized. Different types of basic estimates of the functionals are used simultaneously—an estimate based on collisions, an estimate based on the range, and the method of mathematical expectations. The program MARS11 uses not only these estimates but also the complete arsenal of means for reducing the dispersion: "splitting" and "roulette," synthesis with analytic solutions, exponential transformation, and so forth. The problem of neutron transport in the range of energies 0.025 eV $< E <$ 10 MeV is solved, depending on the problem, by the Monte Carlo method or the discrete ordinate method.

The tree of trajectories is constructed in accordance with the scheme of Fig. 12d: In each *hA* interaction event at

high energies there is inclusive simulation of the production of one fast nucleon (diffraction nucleon or one from the region $x_F < 0.8$), one charged pion, and one slow cascade nucleon with appropriate statistical weights. The species of hadron (p or n, π^+ or π^-) is sampled. The characteristics of the produced charged pion are used to describe the production of the π^0 at the same vertex. The $K^\pm$ mesons in problems in which they are not specially studied or in which the production of muons is not considered are included in the pion component. Nuclear evaporation is simulated in the simplest way. The investigations showed that such a scheme is the best compromise between the exclusive scheme (Fig. 12a) and the nonbranching process (Fig. 12b), giving the most rapid convergence for calculation of the most varied functionals.

The process of production of muons in a cascade is simulated in accordance with the scheme of Refs. 11 and 84–86. In each inelastic hA collision six hadrons (p, n, $\pi^\pm$, $K^\pm$) with appropriate statistical weights are always generated. At the same vertex the production of direct muons from the decay of the short-lived mesons $\rho, \omega, \varphi, D, J/\psi$ is simulated. In the path to the nuclear interaction or in the decay intervals the decays $\pi^\pm \to \mu^\pm + \nu(\tilde{\nu})$ and $K^\pm \to \mu^\pm + \nu(\tilde{\nu})$ are induced, and the π and K mesons participate with the remaining statistical weight in the further development of the cascade. For the treatment of the passage through matter of the created muons, the bremsstrahlung and deep inelastic nuclear interactions of the muons are directly simulated, while the remaining processes are simulated by a combined method.[1,11,87]

Examples of the use of these methods are given below.

6. DIRECT SIMULATION

Despite the attractive features of the inclusive method of calculating cascades, there are problems that at present can hardly be treated with this method. The most important of these is the calculation of the energy resolution of calorimeters. Because of the fact that inclusive simulation loses the correlations between the particles at a vertex and in a number of cases the conservation laws are satisfied only on the average over many histories, the solution of the problem of the fluctuations of the readings of detectors for individual cascades is beyond the scope of the existing inclusive programs. Here too there is as yet no real alternative to direct exclusive simulation.

The statistical nature of the processes of multiparticle production and of the interaction of particles with matter on the path between discrete events has the consequence that the fluctuations in the development of cascades, especially hadronic ones, can be very appreciable. Results of statistical simulation of electromagnetic and hadronic showers in a calorimeter consisting of cells (2 mm of lead + 1 mm of liquid argon) with a total thickness of 27 radiation lengths are given in Fig. 13 (Ref. 88). The rms deviations of the energy release in the liquid argon of each cell are about 50% for the electron–photon showers but 400% for the hadronic cascade. The various sources of the fluctuations in real calorimeters are analyzed in Ref. 89.

Programs of direct simulation of electron–photon showers are considered in Sec. 4. The exclusive simulation of hadronic cascades with simultaneous calculation of the electron–photon showers, initiated mainly by $\pi^0 \to \gamma\gamma$ decays, is a much more complicated problem. The main programs that realize exclusive simulation of nuclear–electromagnetic cascades in a volume needed for one of the principal applications, hadron calorimetry, are the following:

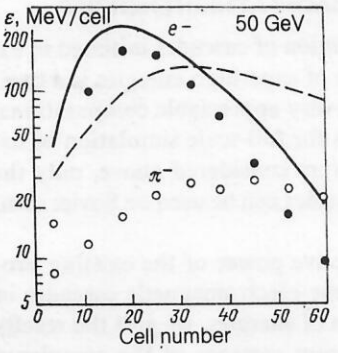

FIG. 13. Mean energy release (points) and the corresponding rms deviations (curves) for electromagnetic and hadronic cascades in a lead–liquid-argon calorimeter at 50 GeV [88]

1) CALOR (Ref. 90), a program based on the intranuclear-cascade model[3,4] and a synthesis of three programs: CALOR = HETC + MORSE + EGS3. This complex simulates best all nuclear effects that are particularly important, for example, in the problem of uranium compensation.[91] The maximal hadron energy recommended by the authors for this program is $E_0 = 30$ GeV,[90,91] although attempts have been made to use it at higher energies;

2) FLUKA82 (Ref. 49), which is a program whose physical model and geometrical module were briefly described in Secs. 2 and 3; it agrees reasonably well with the experimental data[2,92,93] and is designed for calculating hadronic cascades in the energy range 50 MeV $< E <$ 10 TeV. After some improvements in the multiple-production model and the addition of programs for calculating electron–photon showers and the transport of low-energy neutrons, this program could become, despite computational problems, a powerful tool for investigation.

3) GHEISHA (Ref. 50), which has already been considered in the previous sections and is specifically designed for calorimetric problems. It permits reliable exclusive calculation of nuclear–electromagnetic cascades at energies $E_0 \leqslant 0.5$ TeV.

At energies of tens of giga-electron-volts the computing time required by these programs is very appreciable and increases linearly with increasing energy.

Also popular are programs that realize the quasiexclusive approach[1] based on construction of a complete hA event using the single-particle differential cross sections and ensuring the energy–momentum conservation law by means of certain clever devices. These are the programs FLUKA (Ref. 45), TATINA (Ref. 27), the program of Ref. 28, and the programs used in cosmic-ray physics.[26] The quasiexclusive approach is completely justified in the first stage in the solution of the problem of fluctuations in a considered facility, enabling one to obtain the basic dependences. However, it is not possible to calculate the fine details of the studied physical process (correlations, etc.) by means of the programs of this group.

7. CALCULATIONS OF CASCADES AT HIGH ENERGIES

The continuous calculation of cascades initiated in extended systems by particles of superhigh energies is a complicated problem requiring very appreciable computational means. Of all the programs for full-scale simulation of hadron–electromagnetic showers considered above, only the programs of the MARS complex can be used on Soviet computers.

To estimate the predictive power of the existing programs for calculating nuclear–electromagnetic cascades in the tera-electron-volt region of energies, we give the results obtained from the most recent versions of the complexes MARS, CASIM, and FLUKA82. The results of the calculations, made as described above in accordance with the very different schemes, are compared with each other and with the available experimental data at energies $E_0 \geqslant 0.2$ TeV. For the comparison, we have selected the following functionals: the spatial distributions $\Phi(\mathbf{r})$ of the hadron fluxes, the densities $S(\mathbf{r})$ of stars (inelastic nuclear interactions at $p > 0.3$ GeV/c), and the energy-release densities $\varepsilon(\mathbf{r})$. The first two quantities determine the yields from the targets, the backgrounds in the experimental facilities, the scales of the radiation shields, and the levels of the induced radioactivity. The distribution $\varepsilon(\mathbf{r})$ determines the structure of the shower detectors, the heating, and the radiation damage of the targets, absorbers, extraction elements of the accelerators, and the superconducting magnets. Many comparisons of calculated and experimental data are made in the studies cited in the previous sections and devoted to particular programs. We give below results obtained most recently. Some of the data are taken from Ref. 2. The characteristic statistical errors of the calculated results are about 10%.

In Figs. 14 and 15, we give the results of calculations in accordance with the programs MARS10 and FLUKA82 of the fluxes of hadrons with energy $E > 35$ MeV and the energy-release density, and we compare them with the experimental data of Ref. 92 for an aluminum cylinder of length 134 cm and diameter 23 cm irradiated by a filamentary beam of 200-GeV protons. In the FLUKA82 calculation, the taget diameter was 30 cm. The hadron flux was determined by the γ activity of the ^{18}F isotope formed in aluminum plates that divided the layered target. The energy release was measured by means of radiophotoluminescent dosimeters placed on the same aluminum plates. In both cases, the spatial distribution of the cascade was reasonably well reproduced by both programs. The computational data, which agree well with each other, lie somewhat below the experimental points, remaining, however, as is noted in Ref. 92, within the limits of the experimental errors.

The results of investigations of the longitudinal and transverse development of hadronic cascades initiated by 300-GeV protons in an x-ray emulsion chamber are shown in Figs. 16–18. The chamber of Ref. 94, which was a calorimeter model, consisted of stacks of x-ray films of five different sensitivities sandwiched between iron (Fig. 16) and lead (Fig. 17) plates. The experimental data, which are given in Ref. 94 in relative units, are normalized at the single point

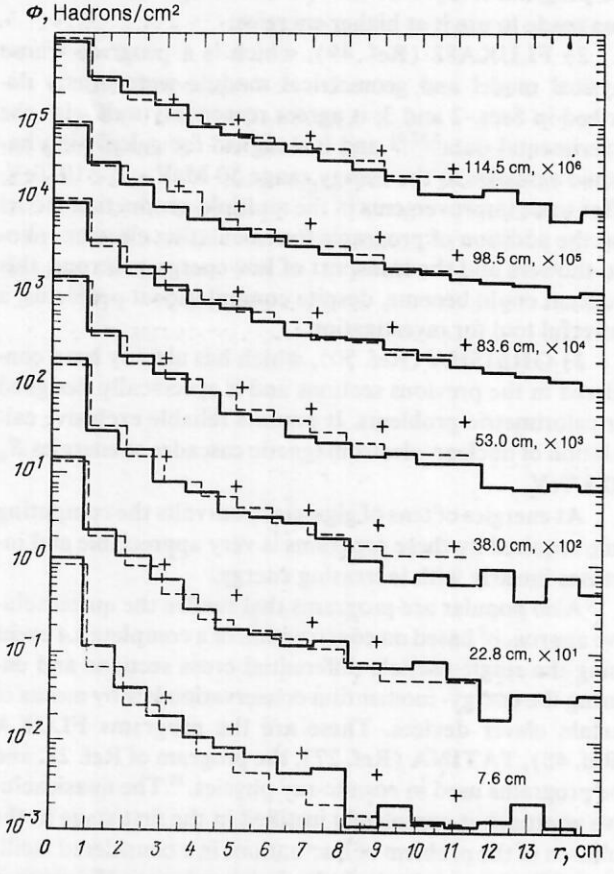

FIG. 14. Hadron fluxes at different thicknesses of an aluminum cylinder exposed to 200-GeV protons as a function of the radius. Calculations: solid histogram, FLUKA82; broken histogram, MARS10; the experimental points (+) are taken from Ref. 92.

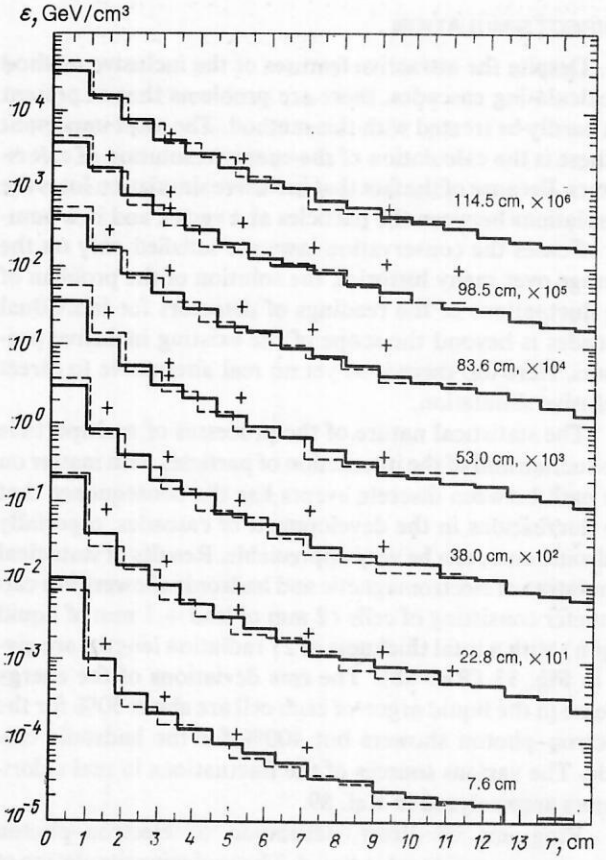

FIG. 15. The same as in Fig. 14 for the energy-release density.

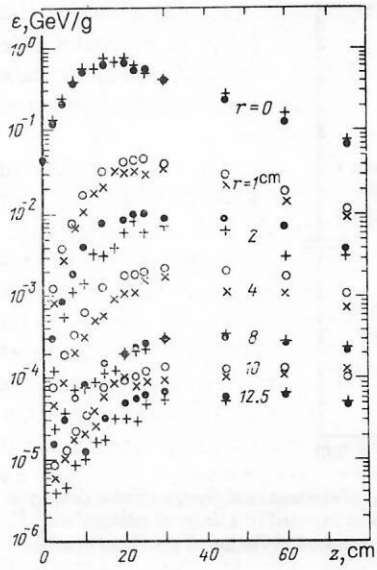

FIG. 16. Spatial distribution of the energy-release density in an x-ray emulsion chamber with iron plates exposed to 300-GeV protons. The plus signs and crosses represent a MARS10 calculation and the black circles and open circles are the experimental data of Ref. 94.

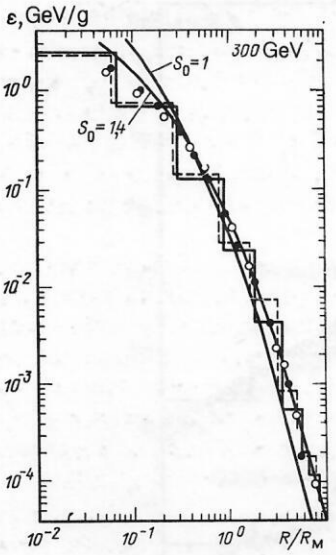

FIG. 18. Radial distribution of energy release in an x-ray emulsion chamber at depth $z = 17.5$ cm for lead (solid histogram and black circles) and $z = 25$ cm for iron (broken histogram and open circles). The histograms were calculated by the program MARS10, the points are from the experiment of Ref. 94, and the continuous curves are the structure functions of the cascade theory of electron–photon showers for two shower ages s_0.

$z = r = 0$ to the results of the MARS10 calculation of the spatial distribution of the energy-release density in x-ray films. In the calculations, all the conditions of the experiment were scrupulously reproduced—the details of the construction of the chamber, the arrangement of the stacks of films of thickness 2.2 mm in 5-mm air gaps, the profile of the primary beam ($\sigma = 0.76$ mm), etc. It can be seen from the figures that in the complete interval of thicknesses and radii the calculation and experiment are in good agreement.

At high energies, the energy release in a nuclear–electromagnetic cascade is determined by the electron–photon showers from $\pi^0 \to \gamma\gamma$ decays, and therefore the radial distribution $\varepsilon(r)$ at the maximum of a hadronic cascade at $E_0 \gtrsim 300$ GeV must agree, especially for heavy materials, with the corresponding distribution of the electromagnetic shower (Refs. 1, 12, 70, and 80). In Fig. 18, such distributions, calculated in accordance with MARS10 for the same chamber, are compared with the experimental data[94] and the results of calculation in accordance with the cascade theory in approximation B for two ages of the shower: $s_0 = 1$ and 1.4. The distance from the cascade axis is here measured in Molière units, which are equal to $R_M = 1.82$ cm for iron and $R_M = 1.65$ cm for lead. As was to be expected for $s_0 = 1.4$, all the results are in good agreement with each other.

As was shown in Ref. 2, the results of calculations of the spatial distribution of the energy-release density and the star density obtained by means of the programs MARS10, CASIM, and FLUKA82 in thick copper targets irradiated with protons of energy 400 and 450 GeV agree well with the experimental data.[95,96] The total number of stars in the target[96] calculated in accordance with these programs is 483, 510, and 443, respectively.

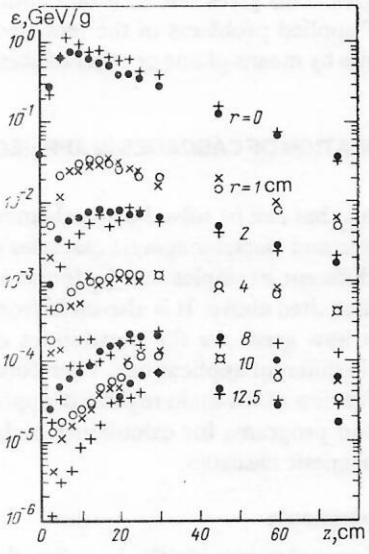

FIG. 17. The same as in Fig. 16 with lead plates.

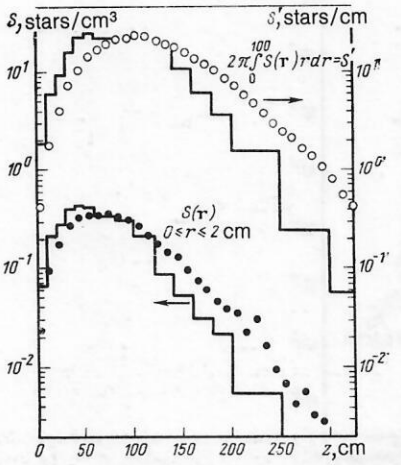

FIG. 19. Longitudinal distribution of the density of stars in a steel absorber; the histograms were calculated by MARS10 and the points by CASIM.

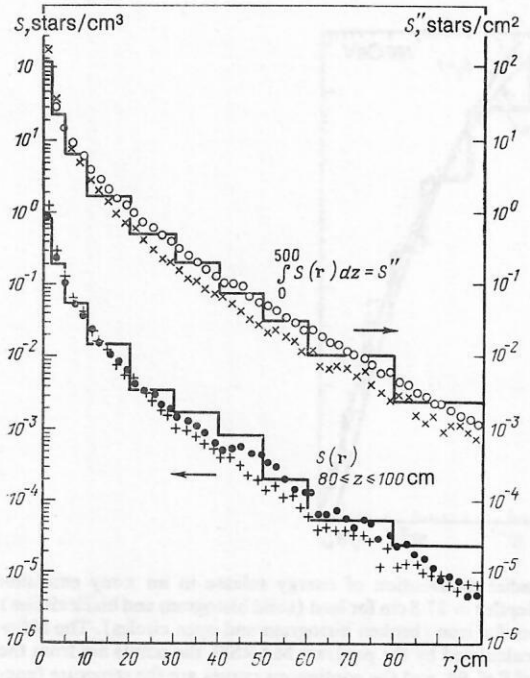

FIG. 20. Radial distribution of the density of stars in a steel absorber, integrated over the thickness (right-hand scale) and at the cascade maximum (left-hand scale) for $E_0 = 10$ TeV. The histograms were calculated by MARSl0, the open circles and black circles by CASIM and the crosses and plus signs by FLUKA82.

The longitudinal profile of a hadronic cascade is fairly sensitive to the method of describing the production of fast nucleons in an hA collision. A detailed consideration of this question in the CASIM and MARS10 programs, special test calculations, and also comparison of Fig. 19 with Figs. 14–18 lead to the conclusion that in the tera-electron-volt region the modified Hagedorn–Ranft model appears to overestimate the yield of nucleons from the nucleus in the fragmentation region. However, as was noted in Ref. 2, this has

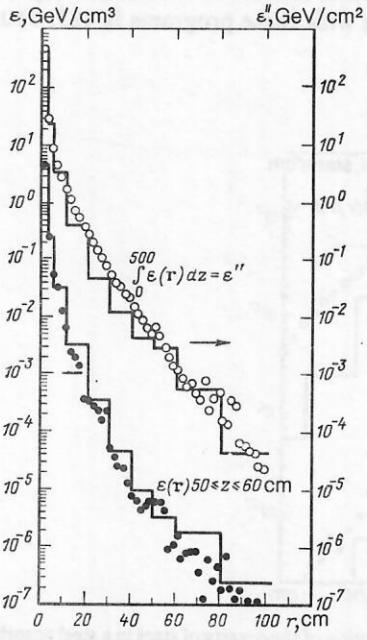

FIG. 21. The same as in Fig. 20 for the energy release density.

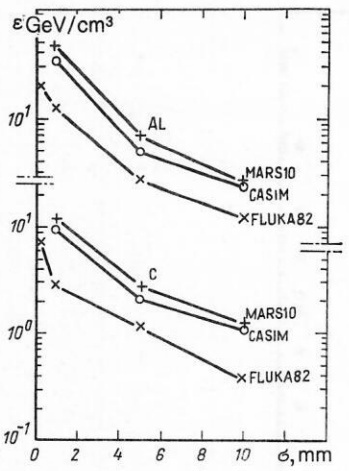

FIG. 22. Results of calculations of the maximal energy-release density in aluminum and graphite absorbers exposed to a beam of protons with $E_0 = 10$ TeV as a function of the standard deviation of the beam density.

hardly any effect on the transverse development of the cascade and the radial distributions $\Phi(\mathbf{r})$ and $S(\mathbf{r})$ calculated by MARS10 and CASIM agree both at the maximum of the cascade and when integrated over the complete block (Fig. 20). The transverse profiles $\varepsilon(\mathbf{r})$ (Fig. 21) also agree well.

In many applications, the quantity $\varepsilon_M = \max \varepsilon(\mathbf{r})$ is important. Its values for cascades initiated by 10-TeV protons incident on absorbers of graphite and aluminum are shown in Fig. 22 as functions of the beam diameter (Gaussian distribution with standard deviation σ). The data obtained in Ref. 97 by means of FLUKA82 are 2–3 times smaller than the results of the calculation of ε_M by MARSl0 and CASIM, which give values that are very nearly equal. The reasons for this were analyzed in detail in Ref. 2. The most important of them is apparently the semiempirical model of an electron–photon shower used in the version of Refs. 49 and 97 of the program FLUKA82.

Thus, despite the significant differences in the models of multiple hadron production and the algorithms for constructing the trajectories, the results obtained by the programs MARS10, CASIM, and FLUKA82 generally agree well with each other and with the existing experimental data in a wide range of energies. This gives one a certain confidence in the solution of applied problems in the tera-electron-volt region of energies by means of one or other of these programs.

8. MATHEMATICAL SIMULATION OF CASCADES IN APPLIED PROBLEMS

The class of problems that can be solved by mathematical simulation of hadronic and electromagnetic cascades is now very large. Many different examples can be found in Ref. 1 and the other studies cited above. It is also clear from the foregoing exposition how great are the possibilities of using existing programs in different applications. Therefore, we shall give only a brief review of the main regions of application of the methods and programs for calculating high-energy nuclear–electromagnetic cascades.

Simulation of physics experiments

The calculations of cascades provide the basis for the stage of planning and optimizing modern experiments in

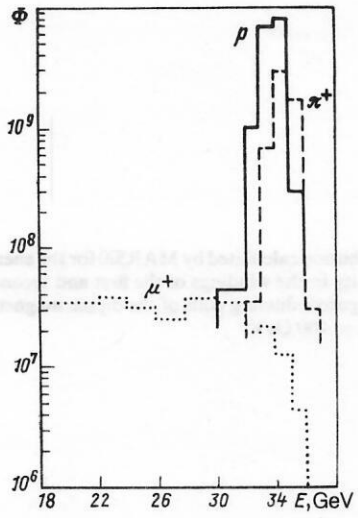

FIG. 23. Calculations by MARSl0–MARSMU of the energy spectra of particles at the center ($r \leqslant 10$ cm) of the tagging station of the tagged-neutrino channel at Serpukhov for a target exposed to 10^{13} protons of energy 70 GeV.

high-energy physics. Computational programs were, for example, effectively used to optimize the yield of antiprotons from targets using a magnetic field,[46] to simulate the production of the characteristic radiation of hadronic atoms when π^- and K^- mesons and Σ^- hyperons are stopped in a target,[77] to optimize the design of the Gamma-1 instrument for high-energy gamma astronomy,[61] and elsewhere. Cascade simulation programs are widely used in the development of experimental facilities and particle channels in operating and planned accelerators at Serpukhov, Fermilab, and CERN. Examples are the optimization of the tagged neutrino channel at Serpukhov (Fig. 23),[98] the optimization of the structure of the neutrino and hadron channels of the UNK,[99,100] the optimization of the Tevatron channels[101] and the design of facilities for UNK experiments. Figure 24 shows the radial distribution of the charged particles at the entrance of the muon spectrometer of the 4π universal calorimetric detector in colliding-beam experiments. Calculations using the program MARSl0 showed that the electron–photon showers, which develop strongly when muons with energy $E > 50$–100 GeV pass through the calorimeter, make the distribution very broad, and as a result it is difficult to identify the muons.

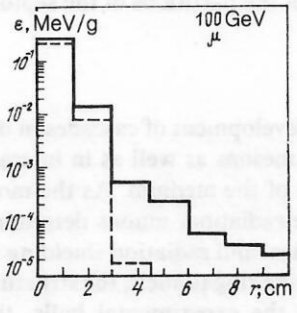

FIG. 24. Energy release from all charged particles (solid histogram) and only from muons (broken histogram) at exit from hadron calorimeter for UNK colliding beam experiments as a function of the distance from the axis of the original motion of the muon.

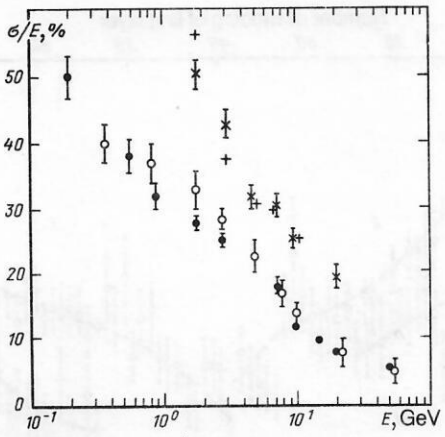

FIG. 25. Energy resolution of two calorimeters. The black circles and open circles are for 0.3-cm U + 0.5-cm Cu + 0.25-cm CH, and the plus signs and crosses are for 0.15-cm Fe + liquid argon. The open circles and crosses are the GHEISHA calculation,[50] and the black circles and pluses are experimental data.[105,106] The results for the second calorimeter are multiplied by 1.5.

Calorimeters

The basic element in the majority of modern experimental detection systems for large accelerators is a calorimeter. It is used to determine the energy of particles or jets, to measure angles, coordinates, and the particle species. Mathematical simulation of hadronic and electromagnetic cascades is universally employed to optimize the structure of the calorimeter in order to improve its characteristics, in the first place the spatial and energy resolution (see, for example, Refs. 1, 89, 91, and 102–104). The results of calculation in accordance with the GHEISHA program[50] of the energy resolution of two types of calorimeter are given in Fig. 25 together with experimental data.[105,106]

New methods of particle detection

The use of the basic features of the development of hadronic and electromagnetic cascades and their subsequent simulation can lead to new ideas about the detection of high-energy particles. Many examples of this can be found in calorimetry; one of them is uranium compensation.[91,106] Another example is the method of detecting particles through the acoustic radiation produced by the development of nuclear–electromagnetic cascades in a dense medium initiated by them.[70] This method was proposed in Ref. 107 for detecting neutrinos of superhigh energies in the DUMAND experiment, in which the huge mass of oceanic water is used as active material of the detector.

Radiative heating of superconducting magnets

The radiative heating of superconducting magnets is one of the most striking problems that can be solved by mathematical simulation of nuclear–electromagnetic cascades in the structural elements of accelerators of the new generation (Refs. 1, 12, 78, and 108–110). Because the allowed level of energy release in the coils is low,[111] the attainment of the desired beam parameters in these accelerator complexes is possible only if special shielding measures are taken to reduce the exposure of the superconducting systems to radiation (Refs. 13–15, 78, 112, and 113). The solution of all three constituents of this problem is based on high-preci-

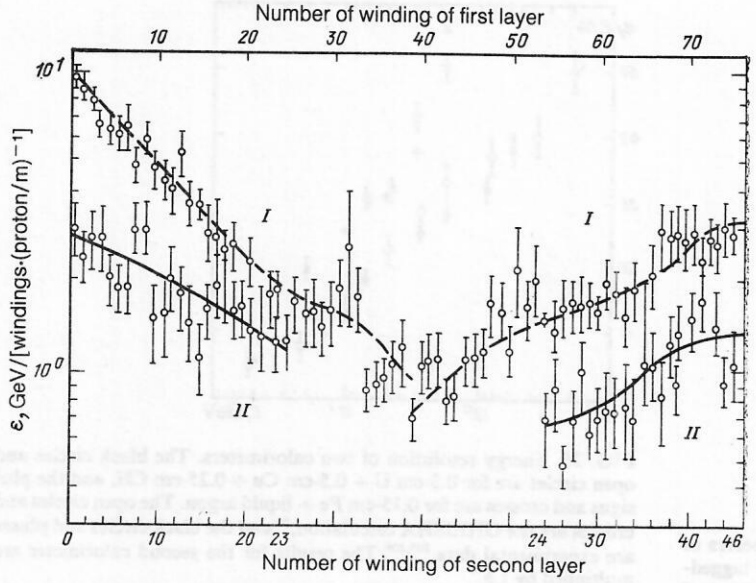

FIG. 26. Distribution calculated by MARS10 for the energy-release density in the windings of the first and second layers of the superconducting coils of the dipole magnets of UNK for $E_0 = 400$ GeV.

sion simulation of the cascades in the accelerator systems:

1) the determination of the admissible energy releases in the coils on the basis of the calculated distributions $\varepsilon(\mathbf{r})$ (Fig. 26) and the maximally permitted proton losses ΔI in the magnetic structure (Fig. 27);

2) the determination of the space–time distributions of the beam losses and of the radiation fields in the elements of the accelerator that then arise (Fig. 28);

3) the determination of shielding measures that will meet the particular considered situation, which, taken together, must ensure a reduction of the radiative energy release in the coils of an arbitrary element to a value lower than the permissible limit (Fig. 28, broken curve).

Such use of the results of calculations of nuclear–electromagnetic cascades (Fig. 29) led to a solution which made it possible to raise by a factor 5 the efficiency of fast resonance extraction of a beam of 800-GeV protons from the superconducting ring of the Tevatron.[15]

Radiative heating

Radiative heating of the elements of accelerator systems and detection facilities occurs when beams of high-energy particles interact with them. Since the planned beam intensities are exceptionally high (up to $6 \cdot 10^{14}$ particles per pulse), numerous macroscopic effects can result from this heating[12]: a raising of the temperature, which complicates the operation of the electric and cooling systems; melting; formation of shock waves, leading to deformation or destruction; reduction of the matter density on the target axis directly in the extraction process, leading to a decrease of the particle yield, and so on. The primary cause of all these effects—energy release in matter associated with the development of the cascades—has been investigated in several studies (Refs. 1, 2, 12, 79, 80, 95, 108, and 114). Figures 30 and 31 show MARS10 calculations of the longitudinal density distributions of the energy release on the axis of targets of length $1.5\lambda_{in}$ made of different materials when a beam of protons with energies 3 and 20 TeV is incident on them. The beam was Gaussian with $\sigma = 0.05$ and 0.2 cm. The results of the calculations of $\varepsilon(\mathbf{r})$ make it possible to optimize the targets and the absorbers.[80] This has resulted in the successful use for a number of years of a system of emergency extraction of beams from the Tevatron with energy up to 800 GeV (Ref. 115); this system was developed on the basis of calculations of cascades by the programs MARS8 (Ref. 80) and CASIM (Ref. 47). A similar system has been developed for the UNK.[116] The calculations[12] of $\varepsilon(\mathbf{r})$ made it possible to propose combined shadow shields of the magnetic and electrostatic septum magnets of the UNK beam extraction systems that reduce the heating of the partitions of the septum magnets by tens of times.

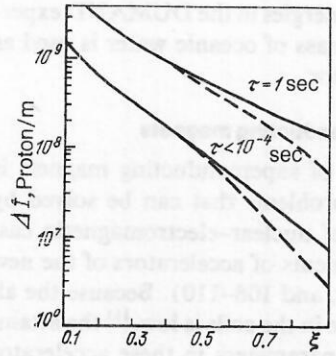

FIG. 27. Maximally permitted density of proton losses in superconducting magnets of the second step in the UNK cycle ($\xi = I/I_{max}$) for two durations of the loss pulses. The broken curve is for the region with maximal magnetic field, and the continuous curve is for the median plane, where $B = 0.875 B_{max}$.

Muons

Muons arise during the development of cascades in decays of long- and short-lived mesons as well as in interactions of neutrinos with nuclei of the medium. As the most penetrating component of the radiation, muons determine the basic size of the technological and radiation shielding in neutrino channels and around the ring tunnels, the structure of the particle channels and the experimental halls, the structure and volume of a significant fraction of the calorimetric 4π detectors for colliding beams, and the background conditions for the majority of other detectors. The results of

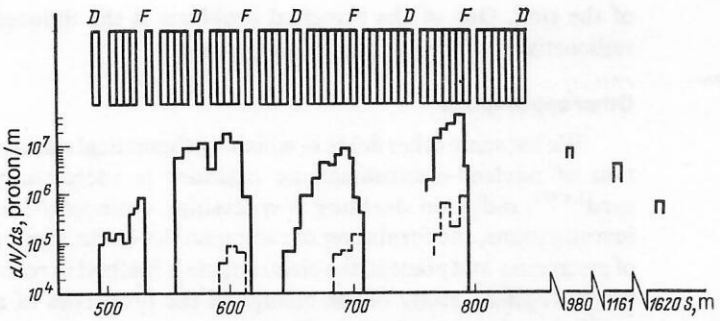

FIG. 28. Distribution of particle losses in superconducting ring electromagnet of the UNK near a straight extraction section in the case of rapid resonance extraction with 99% efficiency of a beam of protons with $E_0 = 3$ TeV. The solid histogram gives the local distortion of the orbit with two mobile collimators; for the broken histogram a third mobile collimator is additionally included (F and D are the focusing and defocusing lenses, respectively).

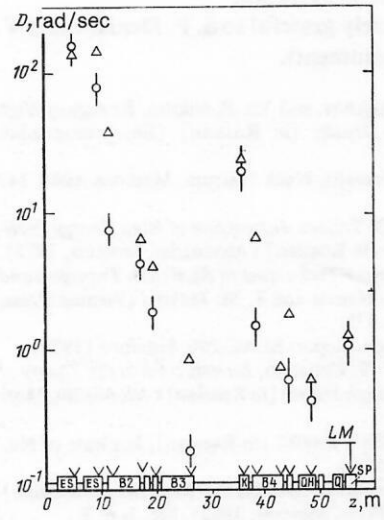

FIG. 29. Readings of ionization chambers situated in magnetic elements of a straight section of the Tevatron in the case of fast resonance extraction of a beam of protons with energy 800 GeV. The open circles represent a MARS10 calculation, and the open triangles are the experimental data.

simulation of the muon distributions in experimental facilities have already been given in Figs. 23 and 24. These data were obtained by inclusive simulation of the production and transport of muons by means of the MARS10–MARSMU program package. In addition, applied problems concerning muons in proton accelerators are solved by means of the Monte Carlo programs MUTRAN (Ref. 11), RING (Ref. 86), the modified CASIM (Ref. 117), and, in some cases, using analytical methods.[118,119]

The following are some examples of calculations: calculation by the MARSMU program of the spectrum of

1) calculation by the MARSMU program of the spectrum of energy losses of muons with mean energy 120 GeV ($\sigma \sim 5$ GeV) after assembly (930 cm of iron and 185 g/cm^2 of air, plastic, etc.) and comparison with calculated and experimental data[120] (Fig. 32);

2) calculation by the MARSMU program of the probability of survival of muons with energies 3 and 20 TeV in ground ($\rho = 2.1$ g/cm^3) (Fig. 33); this provides the basis for the design of absorbers in beam-dump experiments and in the emergency extraction system for the UNK and SSC.

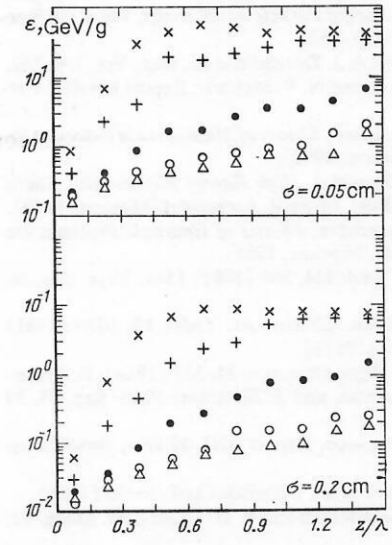

FIG. 30. Longitudinal distribution of energy-release density on the axis of different targets exposed to a beam of protons with energy $E_0 = 3$ TeV and two transverse dimensions. The open triangles are for Be, the black circles for C, the heavy plus signs for Al, the light plus signs for Cu, and the crosses for W.

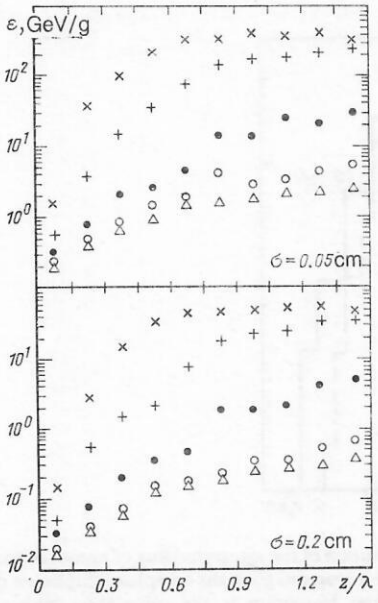

FIG. 31. The same as in Fig. 30 for $E_0 = 20$ TeV.

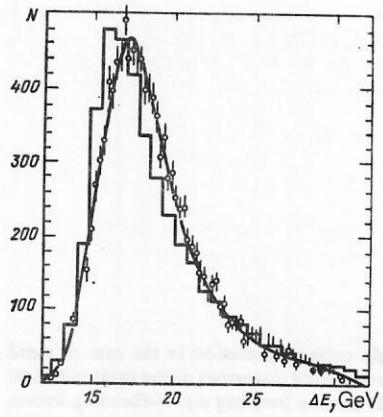

FIG. 32. Distribution with respect to the energy losses for muons with $E_0 \sim 120$ GeV that have passed through a steel assembly. The histogram is the MARSMU calculation, and the curve and the points are, respectively, the calculation and experiment of Ref. 120.

Radiation shielding

This is a traditional application of methods of calculating the passage of radiation through matter. The class of problems that can be solved is here exceptionally large.[121–123] For the existing accelerators, the required shielding thicknesses are appreciable,[122] and it is not possible to solve the problem of radiative transfer by the usual methods. It is necessary to reduce the particle fluxes by a factor 10^5–10^{10} and the shielding configuration is complicated. In such problems it is therefore very effective to use different synthetic methods and modifications of the Monte Carlo method, for example, synthesis of the program MARS11 with a program for numerical solution of the transfer equation by the discrete-ordinate method ROZ-6.[82] The accelerators of the new multi-TeV generation, UNK and SSC, are designed in deep underground tunnels, and this solves the problem of global radiation shielding.[124–126] The classical problems of shielding solved by means of cascade calculations are in this case localized in the experimental halls and the straight sections of the ring. One of the principal problems is the induced radioactivity of the equipment and ground.

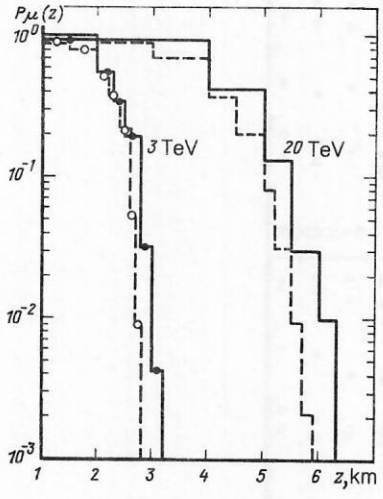

FIG. 33. Longitudinal distribution of the integrated flux of muons of two energies in ground. The solid histogram gives the complete simulation of all processes, and the broken histogram is the calculation without allowance for fluctuations in the production of e^+e^- pairs.

Other applications

We list some other fields in which mathematical simulation of nuclear–electromagnetic cascades is successfully used[1,4,127]: radiation shielding of spaceships, cosmophysical investigations, the formation of radionuclides in the matter of meteorites and planets, the electronuclear method in reactor multipliers, study of the change in the properties of a medium under the influence of intense beams of elementary particles and nuclei, dosimetry and detector sensitivity functions, radiobiology, radiotherapy, and more.

Even this simple list shows how broad is the spectrum of problems that can be effectively solved by means of the existing and continuously improved programs for simulating hadronic and electromagnetic cascades.

The author is sincerely grateful to S. P. Denisov and V. D. Toneev for helpful comments.

[1]A. N. Kalinovskiĭ, N. V. Mokhov, and Yu. P. Nikitin, *Passage of High Energy Particles Through Matter* [in Russian] (Énergoatomizdat, Moscow, 1985).
[2]N. V. Mokhov and J. D. Cossairt, Nucl. Instrum. Methods **A244**, 349 (1986).
[3]V. S. Barashenkov and V. D. Toneev, *Interaction of High Energy Particles and Nuclei with Nuclei* [in Russian] (Atomizdat, Moscow, 1972).
[4]T. W. Armstrong, in: *Computer Techniques in Radiation Transport and Dosimetry*, edited by W. R. Nelson and T. M. Jenkins (Plenum Press, New York, 1980), pp. 311, 373.
[5]R. L. Ford and W. R. Nelson, Report SLAC-210, Stanford (1978).
[6]A. M. Kol'chuzhkin and V. V. Uchaĭkin, *Introduction to the Theory of the Passage of Particles Through Matter* [in Russian] (Atomizdat, Moscow, 1978).
[7]B. E. Shtern, Preprints P-0081, P-0082 [in Russian], Institute of Nuclear Research, Moscow (1978).
[8]Yu. G. Lyutov, in: *New Instruments, Devices and Methods* [in Russian] (Moscow State University Press, Moscow, 1982), Sec. 1, p. 7.
[9]É. V. Bugaev, Yu. D. Kotov, and I. L. Rozental', *Cosmic Muons and Neutrinos* [in Russian] (Atomizdat, Moscow, 1970).
[10]A. Van Ginneken, Preprint Fermilab-Pub-86/33 (1986).
[11]N. V. Mokhov, G. I. Semenova, and A. V. Uzunian, Nucl. Instrum. Methods **180**, 469 (1981).
[12]N. V. Mokhov, Preprint No. 82-168 [in Russian], Institute of High Energy Physics, Serpukhov (1982).
[13]I. S. Baĭshev, M. A. Maslov, and N. V. Mokhov, in: *Proc.of the Eighth All-Union Symposium on Charged Particle Accelerators*, Vol. 2 [in Russian] (JINR, Dubna, 1983), p. 167.
[14]I. S. Baĭshev, V. I. Balbekov, A. I. Drozhdin *et al.*, *ibid.*, Vol. 1, p. 262.
[15]A. I. Drozhdin, M. Harrison, and N. V. Mokhov, Report FN-418, Fermilab (1985).
[16]Yu. P. Nikitin and I. L. Rozental', *Theory of Multiparticle Processes* [in Russian] (Atomizdat, Moscow, 1976).
[17]Yu. P. Nikitin and I. L. Rozental, *High Energy Physics with Nuclei* (Harwood, Chur, 1986) [Russ. original, Atomizdat, Moscow, 1980].
[18]V. S. Murzin and L. I. Sarycheva, *Physics of Hadronic Processes* [in Russian] (Énergoatomizdat, Moscow, 1986).
[19]N. N. Nikolaev, Usp. Fiz. Nauk **134**, 369 (1981) [Sov. Phys. Usp. **24**, 531 (1981)].
[20]Yu. M. Shabel'skiĭ, Fiz. Elem. Chastits At. Yadra **12**, 1070 (1981) [Sov. J. Part. Nucl. **12**, 430 (1981)].
[21]H. U. Bengtsson, Comput. Phys. Commun. **31**, 323 (1984); B. Anderson, G. Gustafson, G. Ingelman, and T. Sjostrand, Phys. Rep. **97**, 33 (1983).
[22]F. E. Paige and S. D. Protopescu, Report BNL-370066, Brookhaven (1985).
[23]C. Buchanan, B. Cox, J. Lach *et al.*, Fermilab-Conf.-86/15 (1986).
[24]V. S. Barashenkov, N. M. Sobolevskiĭ and V. D. Toneev, At. Energ. **32**, 217 (1972).
[25]T. W. Armstrong and K. C. Chandler, Nucl. Sci. Eng. **49**, 110 (1972).
[26]A. N. Dem'yanov, V. S. Murzin, and L. I. Sarycheva, *Nuclear Cascade Processes in Dense Matter* [in Russian] (Nauka, Moscow, 1977).
[27]A. Baronchelli, Nucl. Instrum. Methods **118**, 445 (1974).
[28]A. Grant, Nucl. Instrum. Methods **131**, 167 (1975).

[29]B. B. Levchenko and N. N. Nikolaev, Yad. Fiz. **36**, 453 (1982); **37**, 1016 (1983) [Sov. J. Nucl. Phys. **36**, 265 (1982); **37**, 602 (1983)].
[30]V. S. Barashenkov and N. V. Slavin, Fiz. Elem. Chastits At. Yadra **15**, 997 (1984) [Sov. J. Part. Nucl. **15**, 446 (1984)].
[31]N. S. Amelin and V. S. Barashenkov, Preprint R2-83-770 [in Russian], JINR, Dubna (1983).
[32]N. V. Mokhov, in: *Proc. of the Eighth All-Union Symposium on Charged Particle Accelerators*, Vol. 2 [in Russian] (Nauka, Moscow, 1974), p. 222.
[33]I. S. Baĭshev, S. L. Kuchinin, and N. V. Mokhov, Preprint No. 78-2 [in Russian], Institute of High Energy Physics, Serpukhov (1977).
[34]J. Nyiri, V. V. Anisovich, Yu. M. Shabelsky, and M. M. Kobrinsky, Preprint KFKI-1982-32 (1982).
[35]E. Stenlund and I. Otterlund, Preprint CERN-EP/82-42 (1982).
[36]J. Ranft and J. T. Routti, Part. Accel. **4**, 101 (1972).
[37]B. S. Sychev, A. Ya. Serov, and B. V. Man'ko, Preprint No. 799 [in Russian], MRTI, Moscow (1979).
[38]A. Brenner, D. C. Carey, J. E. Elias *et al.*, Phys. Rev. D **26**, 1497 (1982).
[39]D. S. Barton, C. W. Brandenburg, W. Busza *et al.*, Phys. Rev. D **27**, 2580 (1983).
[40]J. V. Allaby, F. Binon, A. Diddens *et al.*, Report CERN 70-12 (1970).
[41]T. Eichten, D. Haidt, J. B. M. Pattison *et al.*, Nucl. Phys. **B44**, 333 (1972).
[42]N. I. Bozhko, A. A. Borisov, A. S. Vovenko *et al.*, Preprint No. 79-78 [in Russian], Institute of High Energy Physics, Serpukhov (1979).
[43]W. Busza, J. E. Elias, D. F. Jacobs *et al.*, Phys. Rev. Lett. **34**, 836 (1975).
[44]H. W. Bertini, A. H. Culkowski, O. W. Hermann *et al.*, Report ORNL/TM-5710 (1977).
[45]J. Ranft and J. T. Routti, Comput. Phys. Commun. **7**, 327 (1974).
[46]B. V. Chirikov, V. A. Tayurski, H. J. Möhring, and J. Ranft, Nucl. Instrum. Methods **114**, 129 (1977).
[47]A. Van Ginneken, Report FN-272, Fermilab (1975).
[48]H. Grote, R. Hagedorn, and J. Ranft, *Atlas of Particle Production Spectra* (CERN, 1970).
[49]P. A. Aarnio, J. Ranft, and G. R. Stevenson, Report TIS-RP/106-Rev., CERN (1984).
[50]H. Fesefeldt, Report PITHA 85/02, Aachen (1985).
[51]J. Froyland and O. Skontorp, Nucl. Phys. **B68**, 93 (1974).
[52]K. Von Holt, U. Idschok, V. Blobel *et al.*, Nucl. Phys. **B103**, 221 (1976).
[53]W. Ochs and L. Stodolsky, Phys. Lett. **69B**, 225 (1977).
[54]W. Ochs and T. Shimada, Z. Phys. C **4**, 141 (1980).
[55]A. D. Frank-Kamenetskiĭ, *Simulation of Neutron Trajectories for Reactor Design by the Monte Carlo Method* [in Russian] (Atomizdat, Moscow, 1978).
[56]M. A. Maslov and N. V. Mokhov, Preprint No. 85-8 [in Russian], Institute of High Energy Physics, Serpukhov (1985).
[57]R. Brun, M. Caillat, M. Maire *et al.*, Report CERN DD/85/1 (1985); DD/EE/84-1 (1984).
[58]I. S. Baĭshev, N. V. Mokhov, and S. I. Striganov, Yad. Fiz. **42**, 1175 (1985) [Sov. J. Nucl. Phys. **42**, 745 (1985)].
[59]H. Messel and D. F. Crawford, *Electron–Photon Shower Distribution Functions* (Pergamon Press, New York, 1970).
[60]I. S. Baĭshev and N. V. Mokhov, Preprint No. 79-124 [in Russian], Institute of High Energy Physics, Serpukhov (1979).
[61]V. V. Akimov, I. D. Blokhintsev, K. V. Vorob'ev *et al.*, Preprint Pr-684 [in Russian], Institute of Nuclear Research, Moscow (1981).
[62]Ts. A. Amatuni, Preprint EFI-735 (50)-84 [in Russian], Erevan (1984).
[63]H. Hirayama, W. R. Nelson, A. Del Guerra *et al.*, Report SLAC-PUB-3038 (1983).
[64]W. R. Nelson, H. Hirayama, and D. W. O. Royers, Report SLAC-265, Stanford (1985).
[65]A. Van Ginneken, Report FN-309, Fermilab (1978).
[66]A. A. Logunov, M. A. Mestvirishvili, and Nguen Van Hieu, Phys. Lett. **25B**, 611 (1967).
[67]R. P. Feynman, Phys. Rev. Lett. **23**, 1415 (1969).
[68]J. Benecke, T. T. Chou, C. N. Yang, and E. Yen, Phys. Rev. **188**, 2159 (1969).
[69]R. Muradyan, *Self-Similarity (Scaling) in Inclusive Reactions*, R2-6762 [in Russian] (JINR, Dubna, 1972).
[70]O. A. Askariyan, B. A. Dolgoshein, A. N. Kalinovsky, and N. V. Mokhov, Nucl. Instrum. Methods **164**, 267 (1979).
[71]V. V. Uchaĭkin, Zh. Vychisl. Mat. Mat. Fiz. **16**, 758 (1976).
[72]A. V. Plyasheshnikov and K. V. Vorob'ev, Preprint No. 83-12 [in Russian], Institute of High Energy Physics, Alma-Ata (1983).
[73]A. Van Ginneken, Report FN-250, Fermilab (1972).
[74]N. V. Mokhov and V. V. Frolov, At. Energ. **38**, 226 (1975).
[75]S. L. Kuchinin, N. V. Mokhov, and Ya. N. Rastsvetalov, Preprint No. 75-74 [in Russian], Institute of High Energy Physics, Serpukhov (1975).
[76]J. Ranft and N. R. Nelson, CERN Report HS-RP/031/PP (1979).
[77]D. S. Denisov, A. V. Zhelamkov, V. M. Zhelyaznikov *et al.*, Preprint No. 459 [in Russian], Leningrad Institute of Nuclear Physics, Leningrad (1979).
[78]M. A. Maslov and N. V. Mokhov, Part. Accel. **11**, 91 (1980).
[79]N. V. Mokhov and A. Van Ginneken, Report TM-977, Fermilab (1980).
[80]N. V. Mokhov, Report FN-328, Fermilab (1980).
[81]V. P. Kryuchkov, V. N. Lebedev, and N. V. Mokhov, Preprint No. 76-132 [in Russian], Institute of High Energy Physics, Serpukhov (1976).
[82]I. L. Azhgireĭ, I. A. Kurochkin, and N. V. Mokhov, in: *Abstracts of Papers at the Fourth All-Union Scientific Conference on the Shielding of Nuclear Technical Facilities from Ionizing Radiations* [in Russian] (Tomsk, 1985), p. 8.
[83]K. L. Brown and Ch. Iselin, Report CERN 74-2, Geneva (1974).
[84]N. V. Mokhov, Preprint No. 76-64 [in Russian], Institute of High Energy Physics, Serpukhov (1976).
[85]G. I. Britvich, N. V. Mokhov, and A. V. Uzunyan, Preprint No. 76-66 [in Russian], Institute of High Energy Physics, Serpukhov (1976).
[86]M. A. Maslov, N. V. Mokhov, and A. V. Uzunian, Nucl. Instrum. Methods **217**, 419 (1983).
[87]N. V. Mokhov, S. I. Striganov, and A. V. Uzunyan, Preprint No. 80-56 [in Russian], Institute of High Energy Physics, Serpukhov (1980).
[88]T. Jensen, J. D. Amburgey, and T. A. Gabriel, Nucl. Instrum. Methods **143**, 429 (1977).
[89]U. Amaldi, Phys. Scr. **23**, 409 (1981).
[90]T. A. Gabriel, J. D. Amburgey, and B. L. Bishop, Report ORNL/TM-5619, Oak Ridge (1977).
[91]Workshop on Compensated Calorimetry, Report CALT-68-1305, Pasadena (1985).
[92]G. R. Stevenson, P. A. Aarnio, A. Fasso *et al.*, Report TIS-RP/158/PP, CERN (1985); Nucl. Instrum. Methods **A245**, 323 (1986).
[93]J. Ranft, P. A. Aarnio, and G. R. Stevenson, Report TIS-RP/156/CF, CERN (1985).
[94]Y. Muraki, K. Kasahara, T. Yuda *et al.*, Nucl. Instrum. Methods **A236**, 47 (1985).
[95]P. Sievers, Report TM-SPS/ABT/77-1, CERN (1977).
[96]G. R. Stevenson, Report TIS-RP/IR/84-12, CERN (1977).
[97]A. Fasson, K. Goebel, M. Höfert *et al.*, Report TIS RP/IR/84-20, CERN (1984).
[98]I. S. Baĭshev, A. P. Bugorskiĭ, S. P. Denisov *et al.*, in: *Proc. of the Ninth All-Union Symposium on Charged Particle Accelerators*, Vol. 2 [in Russian] (Dubna, 1985), p. 303.
[99]V. V. Ammosov, A. P. Bugorskiĭ, S. P. Denisov *et al.*, in: *Proc. of the Symposium: Physics Investigations Using the Accelerator and Storage Facility of the Institute of High Energy Physics* [in Russian] (Serpukhov, 1982), p. 26.
[100]V. V. Ammosov, V. V. Vasil'ev, V. I. Garkusha *et al.*, in: *Abstracts of Papers at the 13th International Conference on High Energy Particle Accelerators* [in Russian] (Novosibirsk, 1986), p. 195.
[101]*Direct Neutral Lepton Facility* (Fermilab, 1985).
[102]Yu. D. Prokoshkin, Preprint No. 79-148 [in Russian], Institute of High Energy Physics, Serpukhov (1979).
[103]C. W. Fabjan and T. Ludlam, Report EP/82-37, CERN (1982).
[104]I. S. Baĭshev, N. V. Mokhov, and V. K. Semenov, Preprint No. 85-36 [in Russian], Institute of High Energy Physics, Serpukhov (1985).
[105]O. Botner, S. Dagan, C. W. Fabjan *et al.*, IEEE Trans. Nucl. Sci. **NS-28**, 510 (1981).
[106]C. W. Fabjan, W. Struczinski, W. J. Willis *et al.*, Nucl. Instrum. Methods **141**, 61 (1977).
[107]G. A. Askar'yan and B. A. Dolgoshein, Pis'ma Zh. Eksp. Teor. Fiz. **25**, 232 (1977) [JETP Lett. **25**, 213 (1977)].
[108]N. V. Mokhov, Zh. Tekh. Fiz. **49**, 1254 (1979) [Sov. Phys. Tech. Phys. **24**, 694 (1979)].
[109]R. Dixon, N. V. Mokhov, and A. Van Ginneken, Report FN-327, Fermilab (1980).
[110]L. N. Zaĭtsev, Fiz. Elem. Chastits At. Yadra **11**, 525 (1980) [Sov. J. Part. Nucl. **11**, 201 (1980)].
[111]M. A. Maslov and N. V. Mokhov, Preprint No. 81-128 [in Russian] Institute of High Energy Physics, Serpukhov (1981); in: *III ICFA Workshop* (Protvino, 1981), p. 3.
[112]A. I. Drozhdin, M. A. Maslov, N. V. Mokhov *et al.*, in: *Proc. of the Ninth All-Union Symposium on Charged Particle Accelerators*, Vol. 2 [in Russian] (Dubna, 1985), p. 368.
[113]A. I. Drozhdin, M. A. Maslov, N. V. Mokhov *et al.*, in: *Abstracts of*

Papers at the Tenth International Conference on High Energy Particle Accelerators [in Russian] (Dubna, 1986), p. 137.
[114]I. S. Baĭshev and S. L. Kuchinin, in: *Proc. of the Seventh All-Union Symposium on Charged Particle Accelerators*, Vol. 2 [in Russian] (Dubna, 1981), p. 172.
[115]J. Kidd, N. V. Mokhov, T. Murphy *et al.*, in: *Proc. of the Particle Accelerator Conference*, Vol. 2 (IEEE, 1981), p. 2774.
[116]I. S. Baĭshev, V. A. Vasil'ev, G. G. Gurov *et al.*, in: *Proc. of the Eighth All-Union Symposium on Charged Particle Accelerators*, Vol. 1 [in Russian] (Dubna, 1983), p. 268.
[117]W. R. Nelson, T. M. Jenkins, G. R. Stevenson *et al.*, Report SLAC-PUB-3043-CERN TIS-RP/100/PP (1983).
[118]R. G. Alsmiller, F. S. Alsmiller, J. Barish *et al.*, Report CERN-71-16, Vol. 2 (1971), p. 601.
[119]G. R. Stevenson, Report CERN HS-RP/IR/81-28 (1981).
[120]R. Kopp, A. Argento, Benvenuti et al., Report CERN-EP/85-08 (1985).
[121]V N. Lebedev, N. V. Mokhov, and B. S. Sychev, in: *Problems of Radiation Dosimetry and Shielding*, edited by V. K. Sakharov (Atomizdat, Moscow, 1979), No. 18, p. 152.
[122]J. D. Cossairt, N. V. Mokhov, and C. T. Murphy, Nucl. Instrum. Methods **197**, 465 (1982).
[123]V. N. Lebedev and N. V. Mokhov, in: *Abstracts of Papers at the Fourth All-Union Scientific Conference on the Shielding of Nuclear Technical Facilities from Ionizing Radiations* [in Russian] (Tomsk, 1985), p. 5.
[124]Workshop on SSC Environmental Radiation, SSC-R-1016, Berkeley (1985).
[125]L. W. Jones, Report UM HE 86-2, SSC-54, Michigan (1986).
[126]I. L. Azhgireĭ, I. S. Baĭshev, I. A. Kurochkin *et al.*, in: *Abstracts of Papers at the Tenth International Conference on High Energy Particle Accelerators* [in Russian] (Dubna, 1986), p. 154.
[127]V. S. Barashenkov, Fiz. Elem. Chastits At. Yadra **9**, 1151 (1978) [Sov. J. Part. Nucl. **9**, 452 (1978)].

Translated by Julian B. Barbour